

## 21. SITE 945<sup>1</sup>

### Shipboard Scientific Party<sup>2</sup>

#### HOLE 945A

**Date occupied:** 17 May 1994

**Date departed:** 18 May 1994

**Time on hole:** 17 hr, 30 min

**Position:** 6°57.019'N, 47°55.732'W

**Bottom felt (drill pipe measurement from rig floor, m):** 4147.5

**Distance between rig floor and sea level (m):** 11.35

**Water depth (drill pipe measurement from sea level, m):** 4136.1

**Penetration (m):** 75.50

**Number of cores (including cores having no recovery):** 8

**Total length of cored section (m):** 75.50

**Total core recovered (m):** 74.75

**Core recovery (%):** 99

**Oldest sediment cored:**

Depth (mbsf): 75.50

Nature: Silty clay

Earliest age: Pleistocene

**Principal results:** Site 945 (proposed Site AF-25) is located in the main (Amazon) channel of the Amazon Fan, near the transition from the middle to the lower fan. By sampling in the channel we expected to sample the coarsest sediment transported to the site by latest Pleistocene turbidity currents. The channel is incised, with the channel floor up to 45 m below the levee crest. Site 946, 1.2 km to the east, sampled the adjacent levee of this channel to characterize overflow events, as well as deeper layers that underlie both the channel and levee.

The site was selected from a *Conrad* seismic-reflection profile (C2514; 0217UTC on 18 Dec. 1984). The precise position was determined by a pre-site seismic and a 3.5-kHz survey from *JOIDES Resolution*.

Hole 945A was cored by APC to 75.5 mbsf and recovered 74.75 m (99.0%). Only partial strokes were achieved on the three deepest cores, and some sand appears to have been sucked in. There was gas expansion in many cores. Methane was found throughout the hole, but higher hydrocarbons were not detected. A 50-cm-thick zone of honeycomb structure in a sand bed at 61 mbsf may indicate the presence of gas hydrates.

Three lithologic units are recognized:

Unit I (0–0.45 mbsf) is a bioturbated Holocene nannofossil-foraminifer clay. An iron-rich crust occurs at the base of the unit.

Unit II (0.45–1.46 mbsf) consists of mottled, slightly bioturbated olive-gray mud.

Unit III (1.46–75.26 mbsf) consists of medium- to thick-bedded sand interbedded with mud and thin-bedded sand and silt. Most of the sand is very fine to fine grained, but some beds contain abundant medium sand with rare to common coarse grains and rare granules. Most sand beds are

graded. Many of the thicker beds contain angular to well-rounded clasts of mud. At the top of the unit is an 8-m-thick sand bed with abundant folded mud clasts. The water content of these clasts is about 10% lower than for normally consolidated mud at this sub-bottom depth and is more typical of sediment at 30 mbsf. The clasts are set in a matrix of medium sand, whereas the upper part of the graded bed is fine sand. Lower in Unit III, layers of organic detritus occur in some sand. An interval of bioturbated mud occurs at 19–20 mbsf. In the lower part of the unit, sand beds appear organized in two thinning-upward sequences, from 76 to 53 mbsf and from 53 to 40 mbsf.

Foraminifers and nannofossils range from abundant to few in Units I and II. The boundary between Ericson Zones Z and Y is near the base of Unit II (1.4 mbsf). Rare nannofossils and foraminifers are found in a few samples from Unit III. *P. obliquiloculata* is absent, suggesting an age <40 ka for the upper part of Unit III that contains foraminifers.

Because of the sandy character of the cores, paleomagnetic results are inconclusive. The major changes in organic carbon, nitrogen, and sulfur content are associated with changes in grain size. Well-sorted fine sand has low contents of all three elements.

Comparison of seismic-reflection profiles and lithology suggests that Unit III can be correlated in detail with similar sand, silt, and mud beds at Site 946. The only possible channel-fill deposit at Site 945 is the 8-m-thick sand bed with abundant mud clasts at the top of Unit III. This bed is lithologically similar to that at 58–63 mbsf at Site 943, which also contains large numbers of mud clasts and was interpreted to represent the first deposit following an avulsion.

## SETTING AND OBJECTIVES

### Introduction

Site 945 (proposed Site AF-25) is located in the main (Amazon) channel of the Amazon Fan, near the transition from the middle to lower fan, at a water depth of 4140 m. By sampling in the channel we expected to sample the coarsest sediment transported to the site by latest Pleistocene turbidity currents that travelled from the Amazon Canyon through the sinuous fan valley. Nearby Site 946 sampled the levee of this channel to characterize overflow events, as well as deeper layers that underlie both the channel and levee.

### Setting

Site 945 is located in the most recently active Amazon Fan channel (Figs. 1 and 2). Seismic records suggest that the fan in this area is built of interfingering seismic units. The thicker, more reflective units appear to correlate with the high-amplitude reflection packet (HARPs) identified up-fan. The thinner, less reflective units appear to be levee deposits and disappear down-fan, resulting in a lower fan dominated by the more reflective units (Flood et al., 1991). The channel geometry and near-surface sedimentation patterns in this area have been determined on the basis of multibeam bathymetric and piston core data (Flood et al., 1991; Pirmez, 1994). Site 945 is located where the most recently active segment of the Amazon Channel branched off from an earlier leveed channel that continues to the west. The levee here is only 18 m thick, so the newer channel appears

<sup>1</sup>Flood, R.D., Piper, D.J.W., Klaus, A., et al., 1995. *Proc. ODP, Init. Repts.*, 155: College Station, TX (Ocean Drilling Program).

<sup>2</sup>Shipboard Scientific Party is as given in the list of participants in the contents.

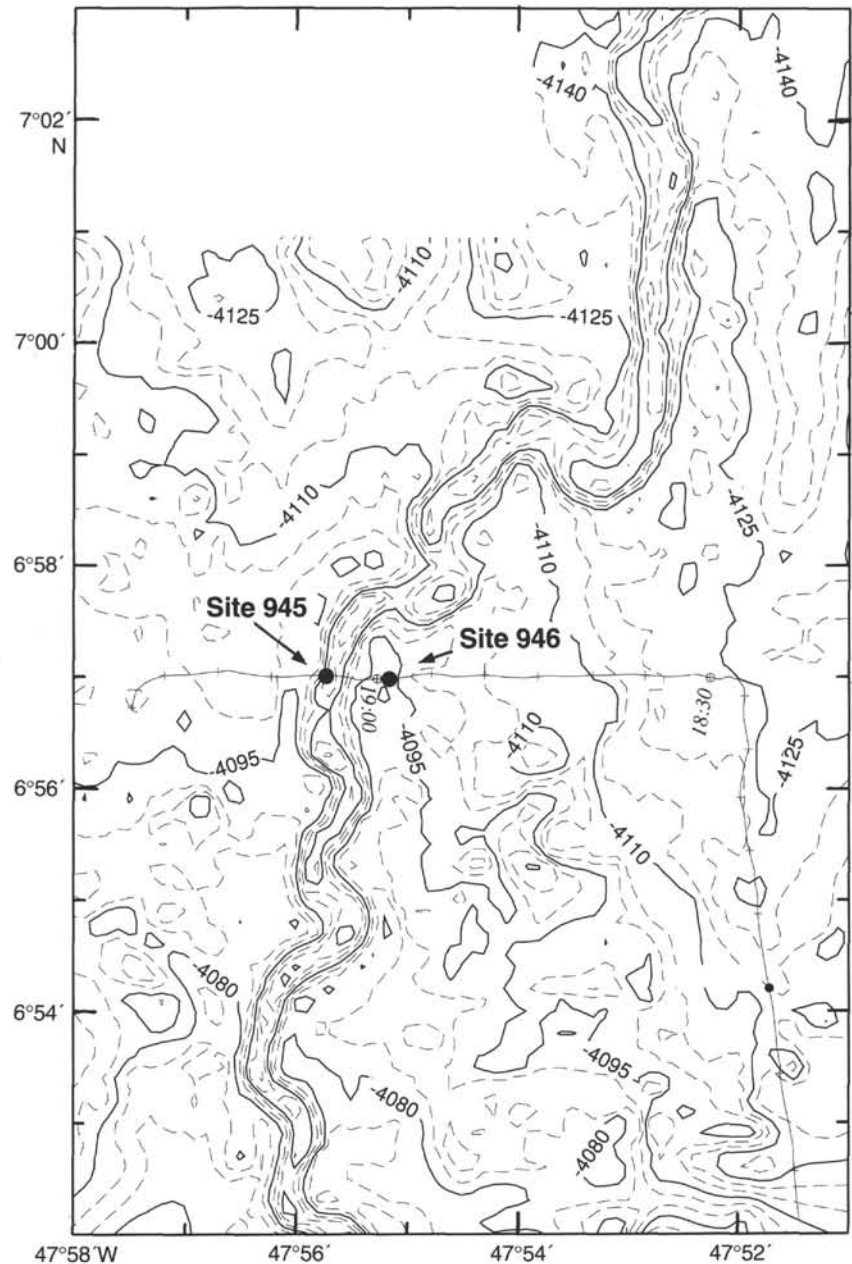


Figure 1. Multibeam bathymetric map of the channel and levee of the Amazon Channel. Locations of Sites 945 and 946 and profiles A-B and C-D are shown. Bathymetry from Flood et al. (1991).

to be incised into sediment that underlies the levee base (Fig. 3). The channel in the vicinity of Site 945 is about 200 m wide and 40 m deep, with a sinuosity of 1.4 and an along-channel gradient of 2.5 m/km (Pirmez, 1994). The site is located in a relatively straight reach of the channel.

The position of Site 945 was chosen on the basis of multibeam bathymetric data near a *Conrad* seismic line (C2514, 0217UTC on 18 Dec. 1984). Our *JOIDES Resolution* seismic profile crossed the site at 1905UTC on 17 May 1994. The position of Site 945 in the channel was verified by the 3.5-kHz profiler and by the length of drill pipe to the mud line; however, the location of the hole relative to its channel walls is unknown.

### Objectives

The principal objectives of coring at Site 945 were:

1. Sampling and characterization of channel-floor sediment in the most recently active channel at the transition from the middle to lower fan.
2. Characterizing the sequence of sediment that fills the channel, especially the relationship of channel fill to underlying units.
3. Sampling sediment related to the earliest stages of channel formation and evolution.
4. Interpretation of turbidity current flow through analysis of turbidity characteristics at this site and, in conjunction with the adjacent Site 946, on the levee crest.

### OPERATIONS

#### Transit: Site 944 to Site 945 (AF-25)

The 60-nmi transit from Site 944 to Site 945 took about 5.6 hr. We conducted a short (~8 nmi) seismic-reflection line to confirm the

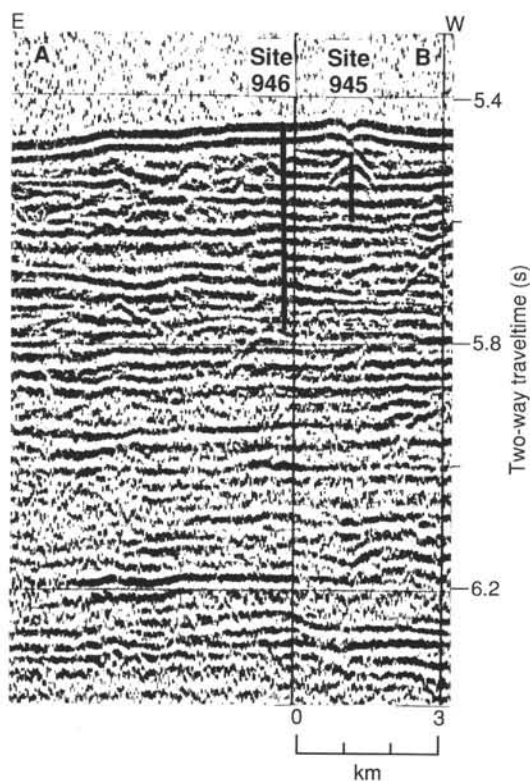


Figure 2. Seismic profile A–B showing a section across the levee of the Amazon Channel and the location of Sites 945 and 946 (JOIDES Resolution 1831–1915 UTC 17 May 1994).

original proposed position. At 1605 hr 17 May, we deployed a beacon at 6°57.012'N, 47°55.724'W.

### Hole 945A

We positioned the bit at 4147.0 mbrf and spudded Hole 945A at 2325 hr 17 May. Core 1H recovered 9.03 m, and the mud line was defined to be at 4147.5 mbrf. The distance from sea level to rig floor, which depends on the ship's draft, was 11.35 m for Hole 945A. Cores 1H through 8H were taken from 4147.5 to 4223.0 m (0–75.5 mbsf) and recovered 74.75 m (99.0%; Table 1). One liner collapsed, and the core barrel only partially stroked while taking Cores 6H, 7H, and 8H. Cores 3H through 8H were oriented using the Tensor tool. No heat-flow measurements were taken. The bit cleared the seafloor at 0823 hr 18 May, and the beacon was recovered at 0927 hr.

## LITHOSTRATIGRAPHY

### Introduction

At Site 945, 75.26 m was cored in one hole with 99% recovery (Fig. 4). Gas was present in some sediment intervals, and gas expansion and escape commonly disrupted the sedimentary structures in many of the silt and sand beds. The sedimentary section is divided into three major lithologic units (Figs. 4 and 5).

### Description of Lithostratigraphic Units

#### Unit I

Interval: 155-945A-1H-1, 0–45 cm  
Age: Holocene  
Depth: 0.00 to 0.45 mbsf

Unit I consists of light yellowish brown calcareous clay (10YR 6/4) with abundant foraminifers and nannofossils. The sediment is moderately bioturbated and slightly color mottled. The base of this unit (interval 945A-1H-1, 42–45 cm; 0.42–0.45 mbsf) contains a distinctive olive brown (2.5Y 4/4), iron-rich crust. This diagenetic, rust-colored crust was analyzed previously and correlated throughout the Amazon Fan and adjacent Guiana Basin (e.g., Damuth, 1977; see "Introduction" chapter, this volume). A black (N 2/0) zone, possibly diagenetic manganese oxide, occurs at 30–32 cm. The character of Unit I is similar to that of the uppermost sediment at most of the other Leg 155 sites.

#### Unit II

Interval: 155-945A-1H-1, 45–146 cm  
Age: Holocene to (?)late Pleistocene  
Depth: 0.45 to 1.46 mbsf

Unit II consists of terrigenous olive gray (5Y 4/2) clay, which grades downhole into olive gray (5Y 5/2) silty clay. The sediment between 0.62 and 1.17 mbsf is stained by small speckles of diagenetic hydrotroilite, which imparts an ephemeral black color (N 2/0) to the sediment (see "Introduction" section in the "Explanatory Notes" chapter, this volume). The carbonate content of Unit II was not measured, but is very low based on weak reaction with 10% HCl. The sediment is slightly bioturbated.

#### Unit III

Interval: 155-945A-1H-1, 146 cm, through -8H-CC, 26 cm  
Age: late Pleistocene  
Depth: 1.46 to 75.26 mbsf

Unit III consists predominantly of thick-bedded sand of variable lithology and depositional origin. The carbonate content is uniformly low (0.6% to 3.2%) throughout. Most of the beds that make up this unit are normally graded from sand to clay (Fig. 5). Beds range in thickness from 1 cm to greater than 9 m; however, medium to thick beds are predominant. The thicknesses of many of the thicker sand beds, especially those in Cores 945A-5H through -8H, are uncertain because the APC core barrel probably achieved incomplete penetration during coring, resulting in "flow-in." Thus, recovered sand intervals may be much thicker than their in-situ bed thicknesses. The sand of Unit III is generally dark olive gray (5Y 3/2) in color and is very fine to fine grained. Some beds contain abundant medium sand with rare to common coarse grains and rare granules. Many of the thicker sand beds contain angular to well-rounded, very dark gray (5Y 3/1) to dark olive gray (5Y 3/2) mud clasts of various sizes and shapes. In some beds, the mud clasts are normally graded, whereas in other beds they appear to be randomly distributed. Some mud clasts are clearly composed of pieces of deformed or folded clay beds. The following is a brief description of typical beds that characterize this unit.

A distinctive thick bed of fine to medium sand occurs at the top of Unit III in interval 945A-1H-2, 0 cm, through -1H-6, 42 cm. This sand bed contains zones of abundant mud clasts of various sizes and shapes in intervals 945A-1H-2, 120 cm, through -1H-3, 40 cm, and -1H-3, 135 cm, through -1H-6, 42 cm, that are angular to well rounded and are composed of dark grayish-brown (2.5Y 3/2) silty clay with black (N 2/0) color banding (Figs. 6 and 7). The color banding clearly shows that the sediment composing the clasts has been folded and deformed either before or during clast formation and transport (Fig. 7). These intervals with clasts are set in a medium to coarse sand matrix; however, in many zones the clasts are so close together that the bed appears to be clast supported. In contrast, the intervals of sand with no clasts are predominantly fine sand.

A thinner bed of fine sand, which contains a similar zone of clay clasts within a matrix of medium to coarse sand, occurs in interval

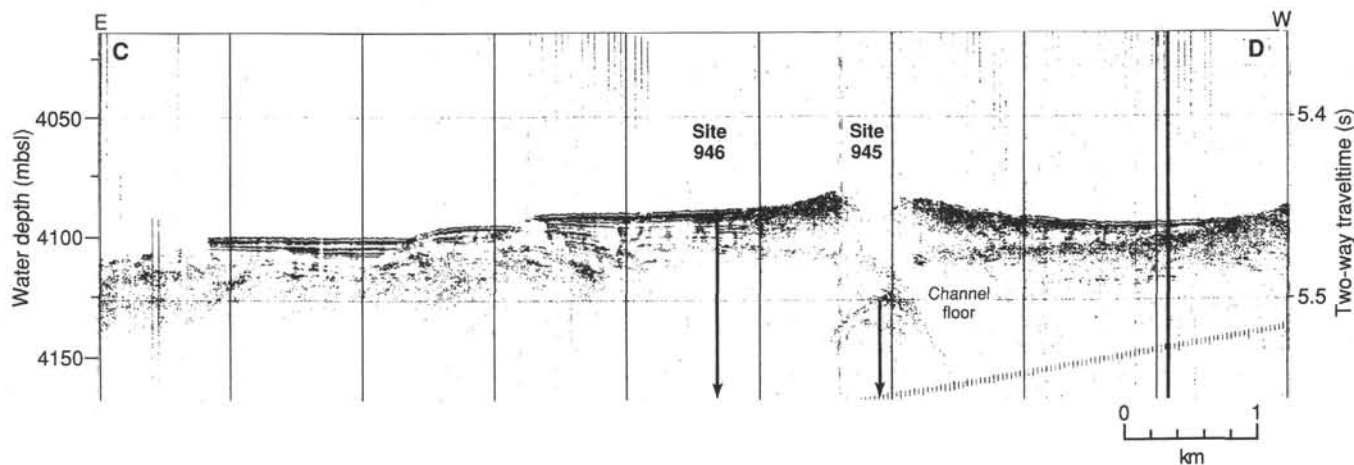


Figure 3. JOIDES Resolution 3.5-kHz profile C-D crossing Sites 945 and 946 (1835–1920 UTC 17 May 1994). Site 945 is located within a channel that is obscured by side echoes. The channel floor is represented by a hyperbolic echo.

Table 1. Site 945 coring summary.

Core	Date (1994)	Time (UTC)	Depth (mbsf)	Length cored (m)	Length recovered (m)	Recovery (%)
155-945A-						
1H	May 18	0345	0.0–9.0	9.0	9.03	100.0
2H	May 18	0500	9.0–18.5	9.5	9.59	101.0
3H	May 18	0605	18.5–28.0	9.5	8.82	92.8
4H	May 18	0715	28.0–37.5	9.5	9.93	104.0
5H	May 18	0815	37.5–47.0	9.5	10.20	107.3
6H	May 18	0925	47.0–56.5	9.5	8.56	90.1
7H	May 18	1025	56.5–66.0	9.5	9.36	98.5
8H	May 18	1135	66.0–75.5	9.5	9.26	97.5
Coring totals				75.5	74.8	99.00

Note: An expanded version of this coring summary table that includes lengths and depths of sections, location of whole-round samples, and comments on sampling disturbance is included on the CD-ROM in the back pocket of this volume.

945A-1H-6, 89 cm, through -2H-1, 65 cm. This interval is separated from the thicker interval described above by a thin deposit of very dark grayish brown (2.5Y 3/2) clay, which is burrowed, intensely color-banded and mottled by hydrotroilite, and contains several silt laminae (Fig. 8). This clay interval may be a large clast within a single thick sand bed composed of both the sand intervals described above (Fig. 5). Physical property measurements within this clay suggest that it may be displaced.

Interval 945A-2H-1, 65 cm, through -2H-5, 108 cm, and interval 945A-3H-2, 44 cm, through -4H-3, 111 cm, consist mainly of a series of thin to thick beds that grade upward from fine sand through silt to clay at the top of each bed (Figs. 5, 9, 10, 11, and 12). The thickest beds in these intervals are 1.6 to 2.5 m thick; however, most beds are thinner than 30 cm. Some of the thinnest beds grade upward from silt into clay, but most of the beds contain very fine to fine sand. A few beds have medium sand at their bases (Fig. 5). Layers of organic detritus occur in some beds and isolated large wood fragments are rare (Fig. 9 and 11). A few beds contain mud clasts of various shapes and sizes (Fig. 10); in most beds, these clasts are rare, but one bed has an interval with numerous large clasts in a fine sand matrix (Fig. 12). Moderately bioturbated and color-mottled dark gray (5Y 4/1) to dark olive gray (5Y 3/2) clay with numerous silt laminae and a few silt beds up to 3 cm thick (interval 945A-2H-5, 108 cm, through -3H-2, 44 cm) separate two intervals of thicker sand beds.

Silt laminae and thin silt and fine sand beds are common in the interval 945A-4H-3, 111 cm, through -4H-7, 88 cm (Figs. 5 and 13); however, a few normally graded beds up to 0.5 m thick are present

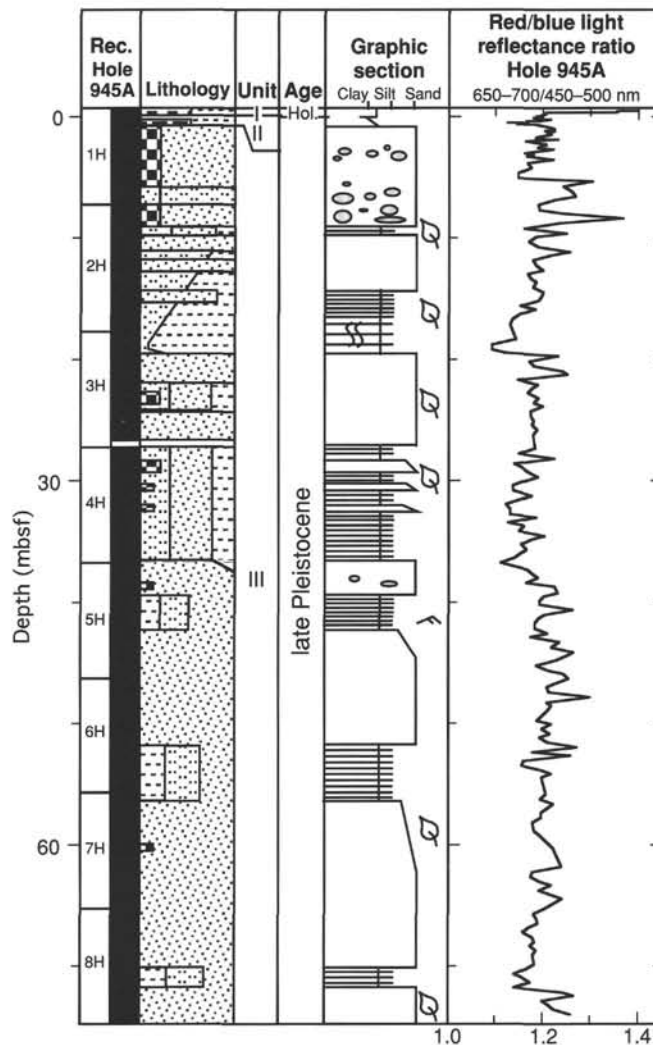


Figure 4. Composite stratigraphic section for Site 945 showing core recovery, a simplified summary of lithology, depths of unit boundaries, age, a graphic section with generalized grain-size and bedding characteristics, and downhole variations in light-reflectance values. The lithologic symbols are explained in Figure 1 of the “Explanatory Notes” chapter, this volume.

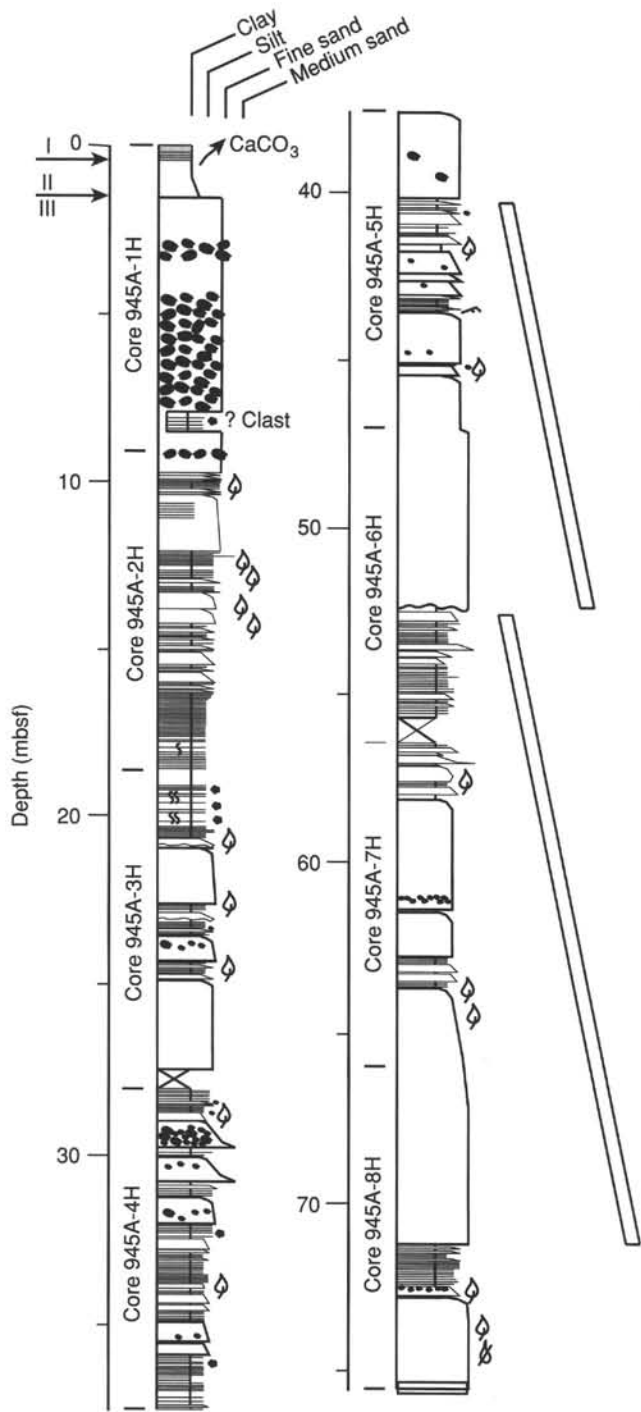


Figure 5. Graphic sedimentological columns for Site 945 showing grain-size variation (width of columns), bed thickness, and sedimentary structures; symbols and preparation of these columns are explained in the "Lithostratigraphy" section of the "Explanatory Notes" chapter, this volume. Slanted open bars mark the limits of possible fining- and thinning-upward cycles. The upper part of the column is shown in the longitudinal profile of the foldout (back pocket, this volume) to show down-fan changes in channel-fill and related mass-failure deposits.

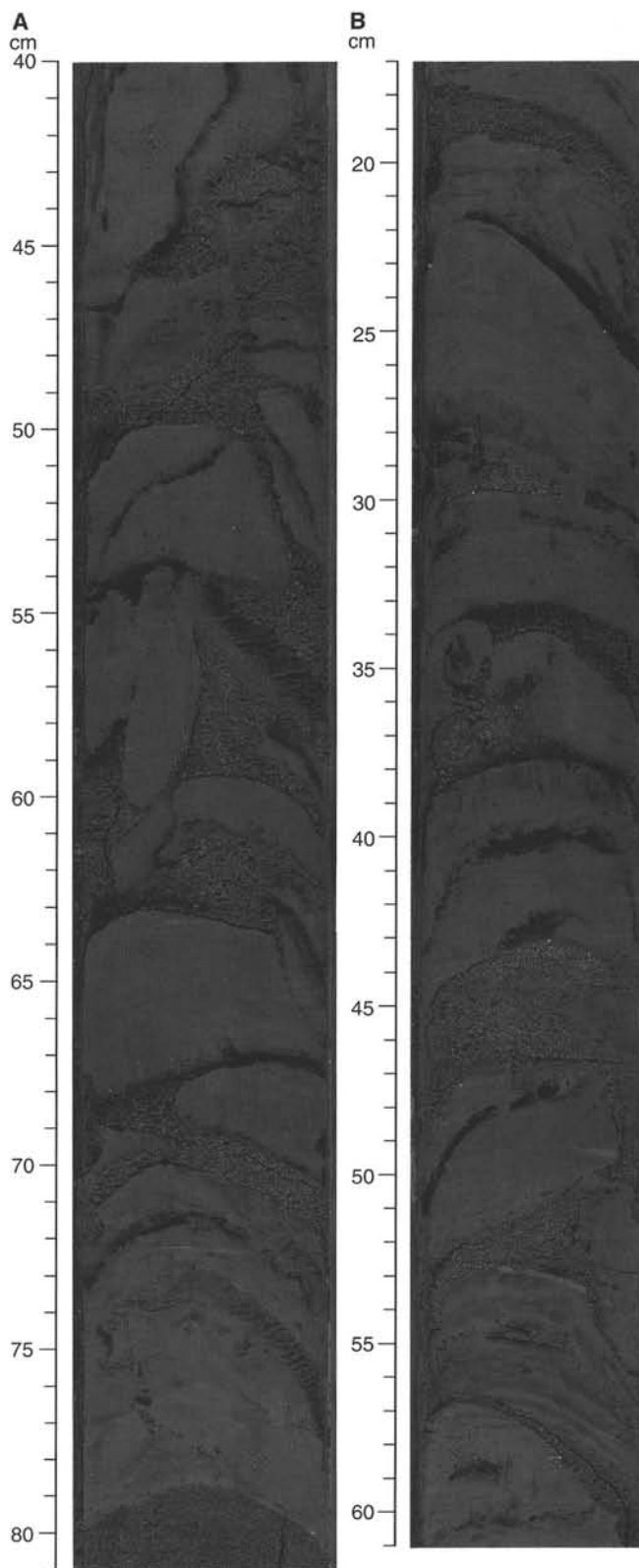


Figure 6. Mud clasts in a matrix of medium to coarse sand near the top of Unit III. A. 155-945A-1H-4, 40–81 cm. B. 155-945A-1H-5, 17–61 cm. Note folded color bands in the clast at 20–24 cm.

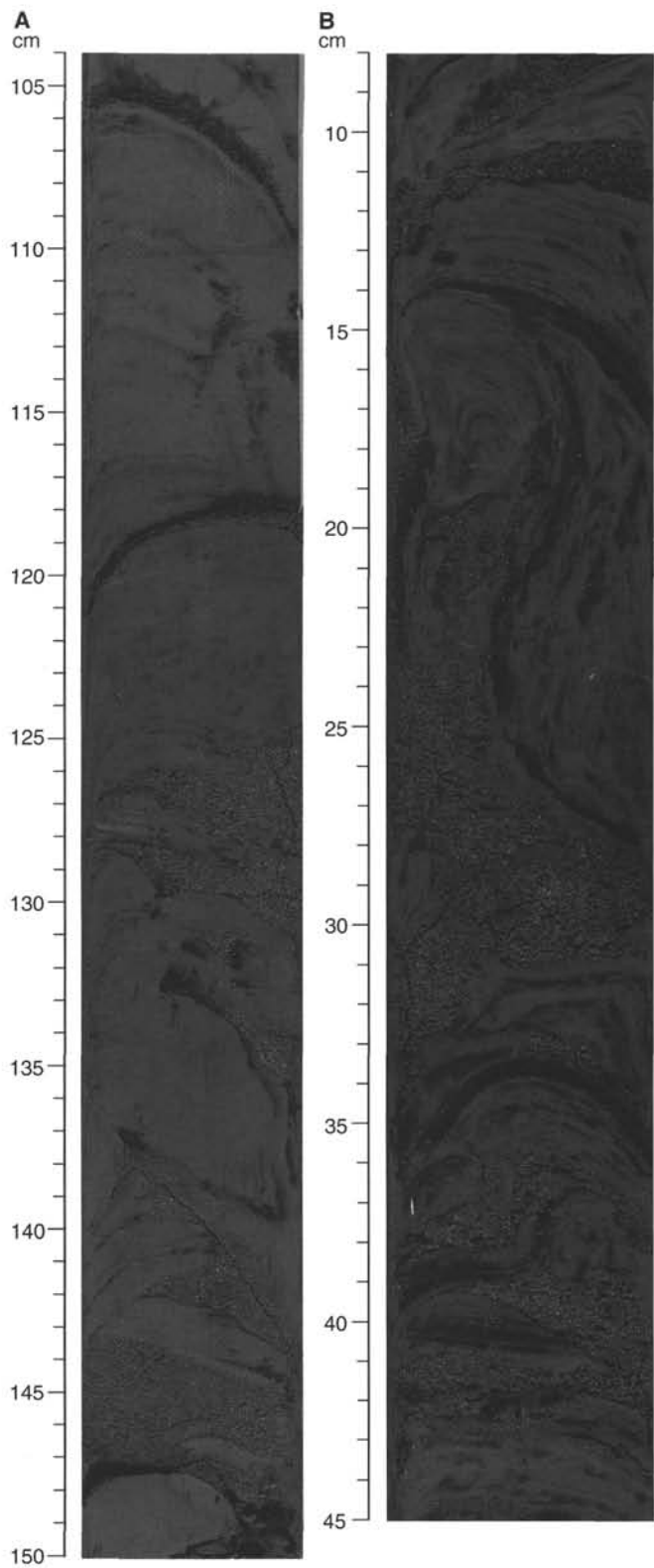


Figure 7. Folded and deformed mud clasts in a medium to coarse sand matrix near the top of Unit III. A. 155-945A-1H-5, 104–150 cm. B. 155-945A-1H-6, 8–45 cm.

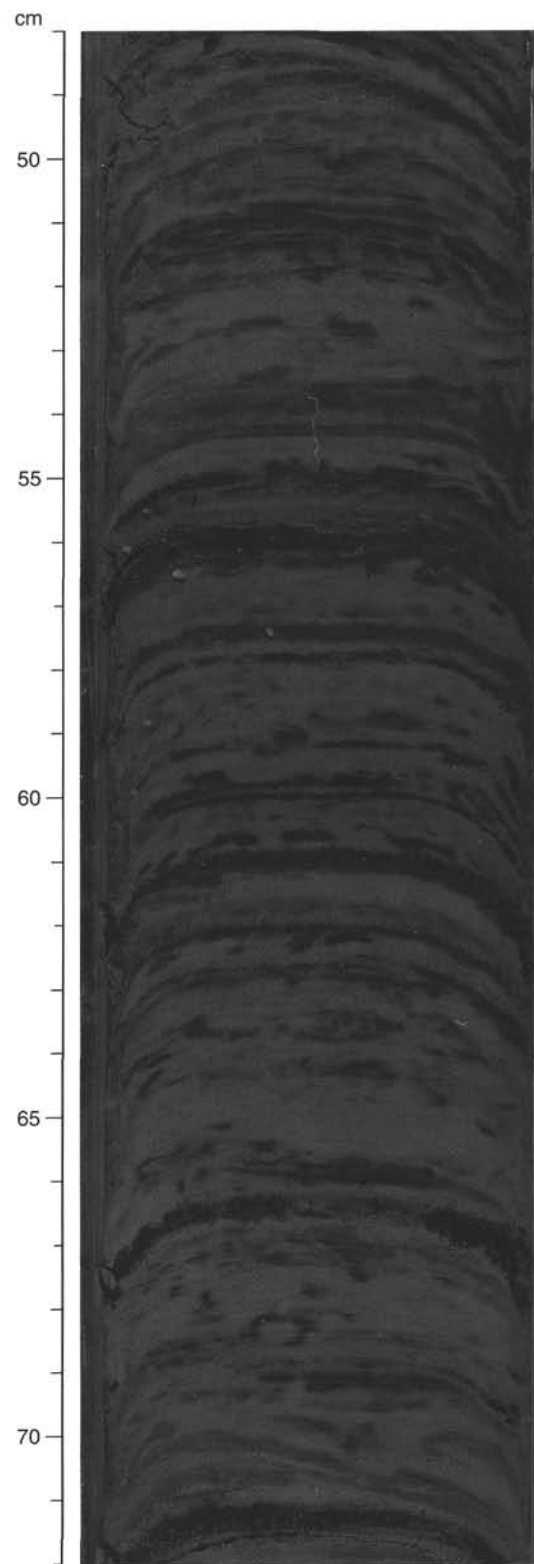


Figure 8. Color-banded and mottled clay with silt laminae and thin beds from Unit III (155-945A-1H-6, 48–72 cm). This interval may be from a large displaced clast (see text and Fig. 5).

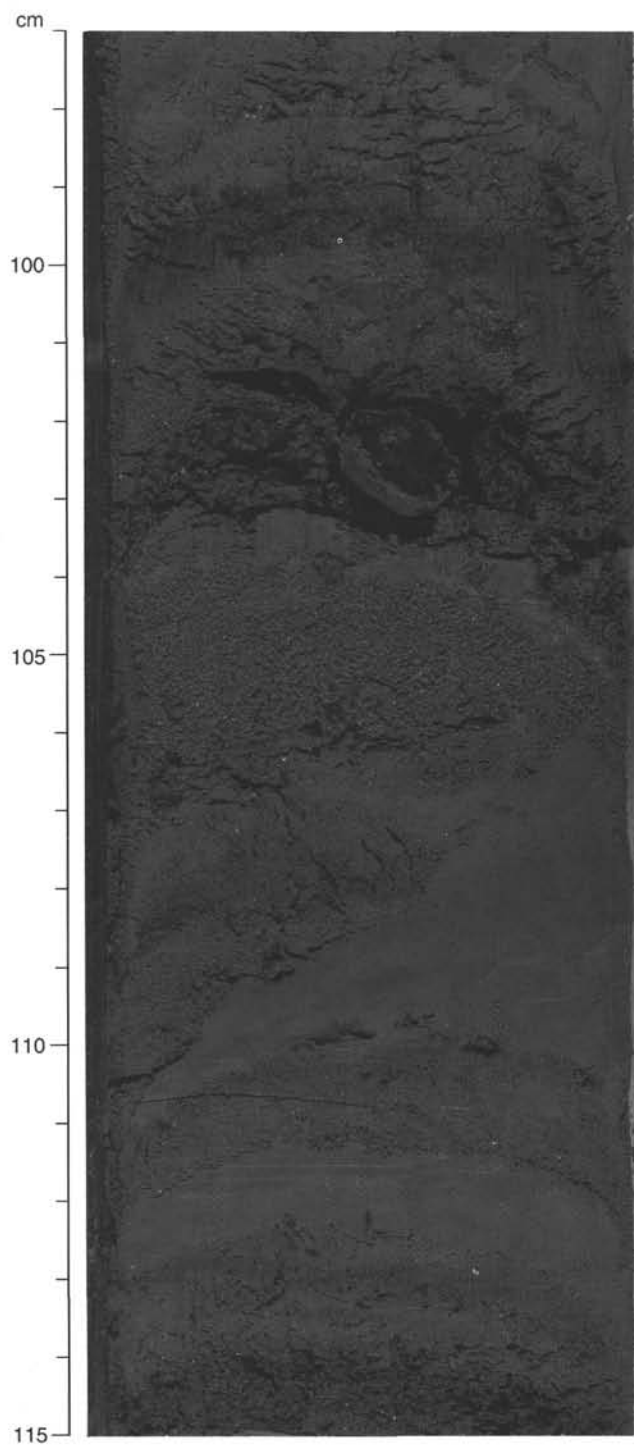


Figure 9. Thin graded beds of silt and fine sand from Unit III (155-945A-2H-3, 97–115 cm). A large wood fragment occurs at 102–103 cm. The origin of the irregular dipping contact from 106 to 111 cm (right to left) is uncertain, but may represent erosional scour.

(Fig. 14). Most sand beds are very fine to fine and grade upward into thin silt and clay at their tops.

Sections 945A-5H-1 through -8H-CC compose the lower half of the cored section and contain several very thick sand beds that might be as thick as 9 m; however, an undetermined portion of each of these beds may be attributable to “flow-in” (Fig. 5). The amount of “flow-

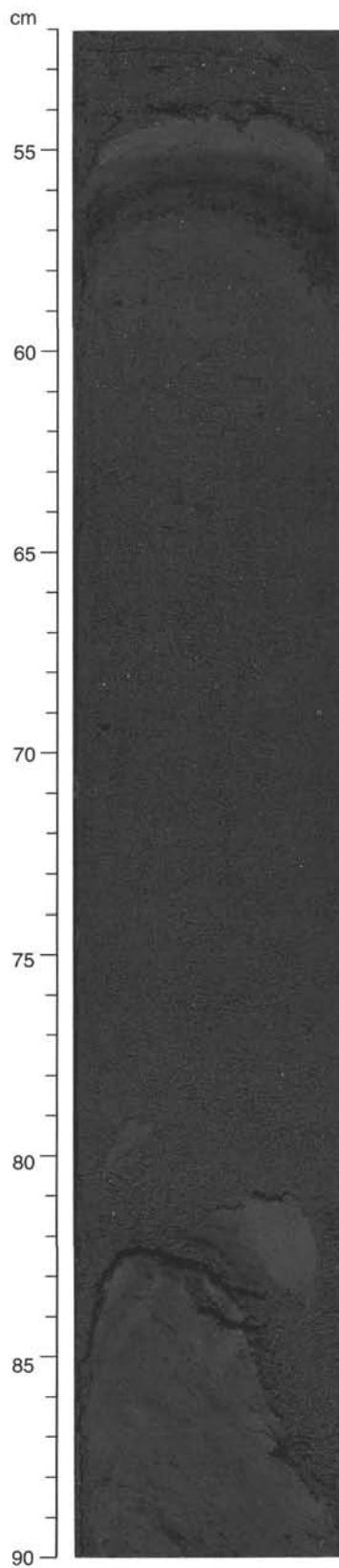


Figure 10. Graded medium bed of sand from Unit III (155-945A-2H-5, 52–90 cm). Fine sand grades into silt and clay at top of bed. Mud clasts occur just above the sharp, irregular base of the bed.

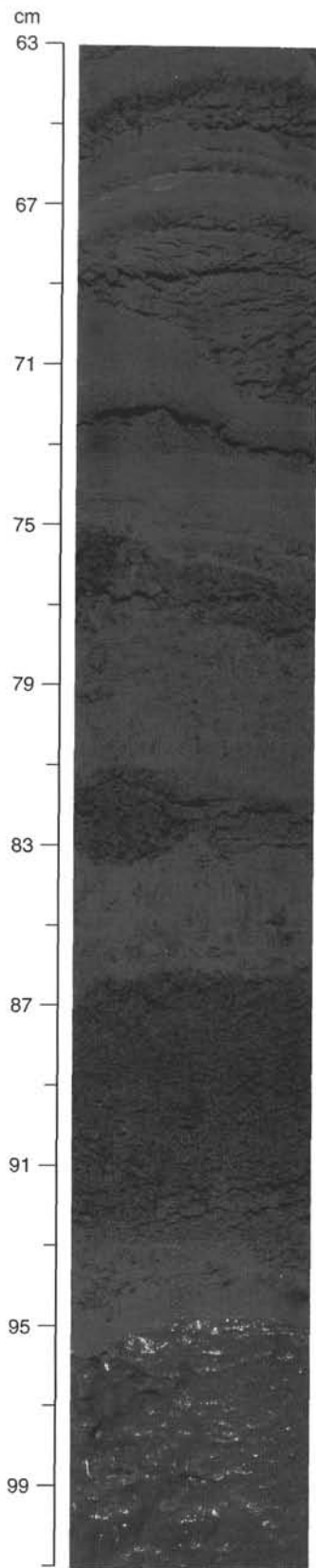


Figure 11. Graded medium bed of sand in Unit III (155-945A-4H-1, 63–101 cm). Top of the bed is at 73 cm; the base is at ~94 cm overlying a very thin clay bed that caps a thick sand bed below. A layer of organic detritus occurs from 86 to 92 cm, and a large wood fragment occurs at 82–83 cm.

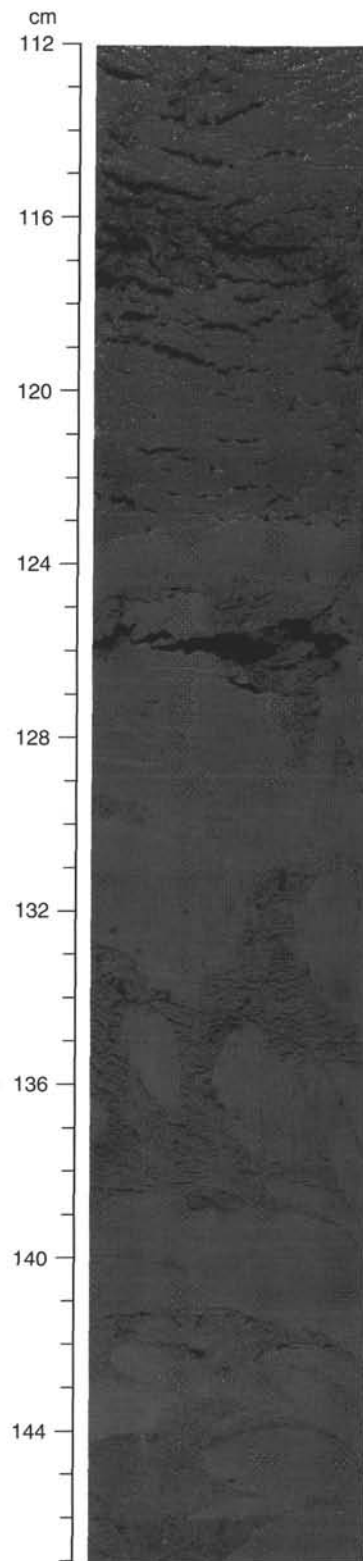


Figure 12. Large mud clasts in the lower portion of the fine sand bed whose top is shown in Figure 11 at ~94 cm (155-945A-4H-1, 112–147 cm). The matrix is fine sand.

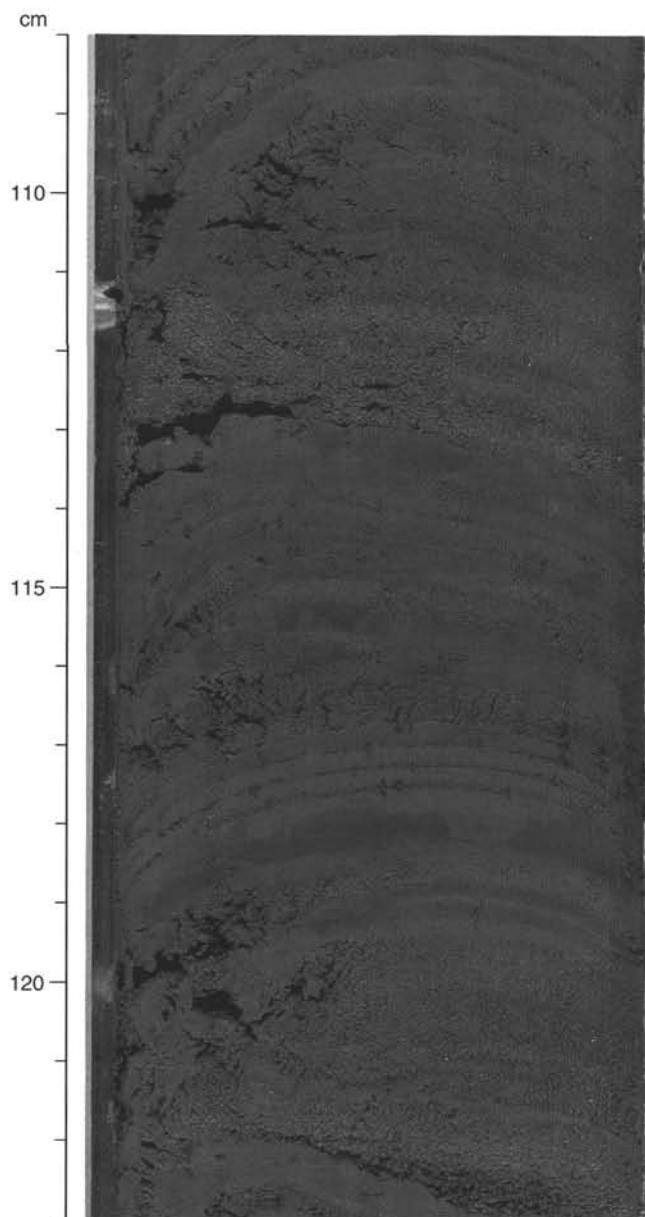


Figure 13. Graded silt laminae and thin, graded, silt and fine sand beds in Unit III (155-945A-4H-4, 108–123 cm).

in” represented in each bed, if any, was not readily apparent during initial megascopic description of the cores. The thick sand bed near the top of this interval extends downhole from Section 945A-5H-1 at 16 cm through -5H-2 at 122 cm and is largely massive, structureless fine sand with common medium-size grains. This sand apparently grades upward into a very thin clay unit at the top. Rare small mud clasts occur in the middle of the sand bed. Beneath this bed are several sand beds of thin and medium thickness. Most are normally graded and have thin intervals of silt and clay at their tops. A few of the thicker beds have rare to common mud clasts. Layers of organic detritus rarely occur.

A bed of predominantly fine sand, approximately 9.5 m thick, comprises interval 945A-5H-5, 15 cm, through -6H-5, 65 cm (Fig 5). This bed is structureless, except at its top where it grades into a few centimeters of thinly laminated silt and clay. The base of the sand is an irregular sharp contact. The upper portion of the bed is fine to very

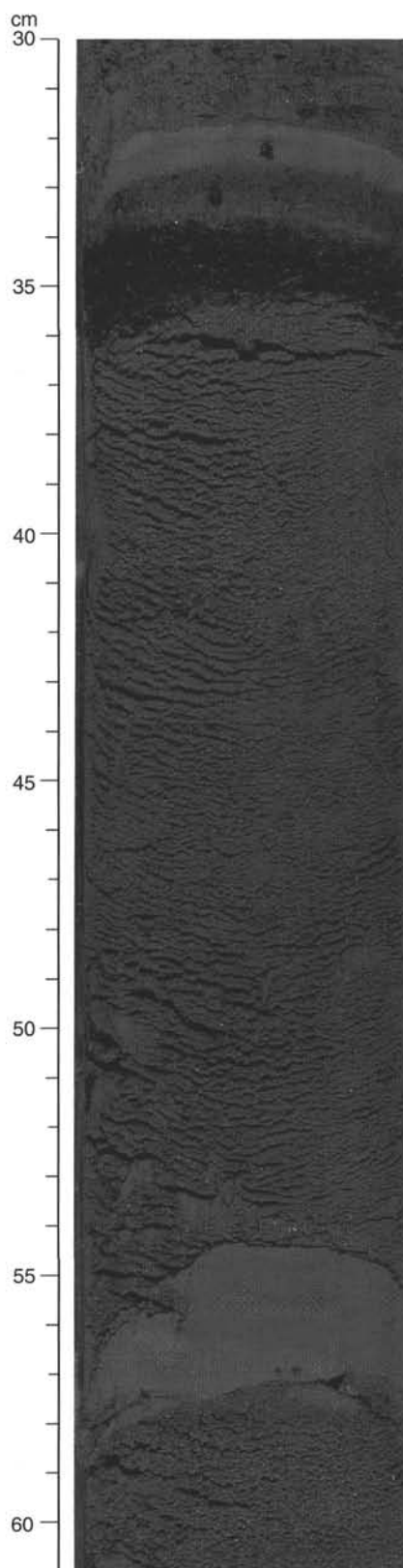


Figure 14. Normally graded sand bed of medium thickness and sharp, erosive base at 54 to 55 cm, from Unit III (155-945A-4H-5, 30–61 cm). A layer of organic detritus is present from 34 to 36 cm near the top of the bed. The bed grades through silt into clay from 32 to 34 cm at top of bed.

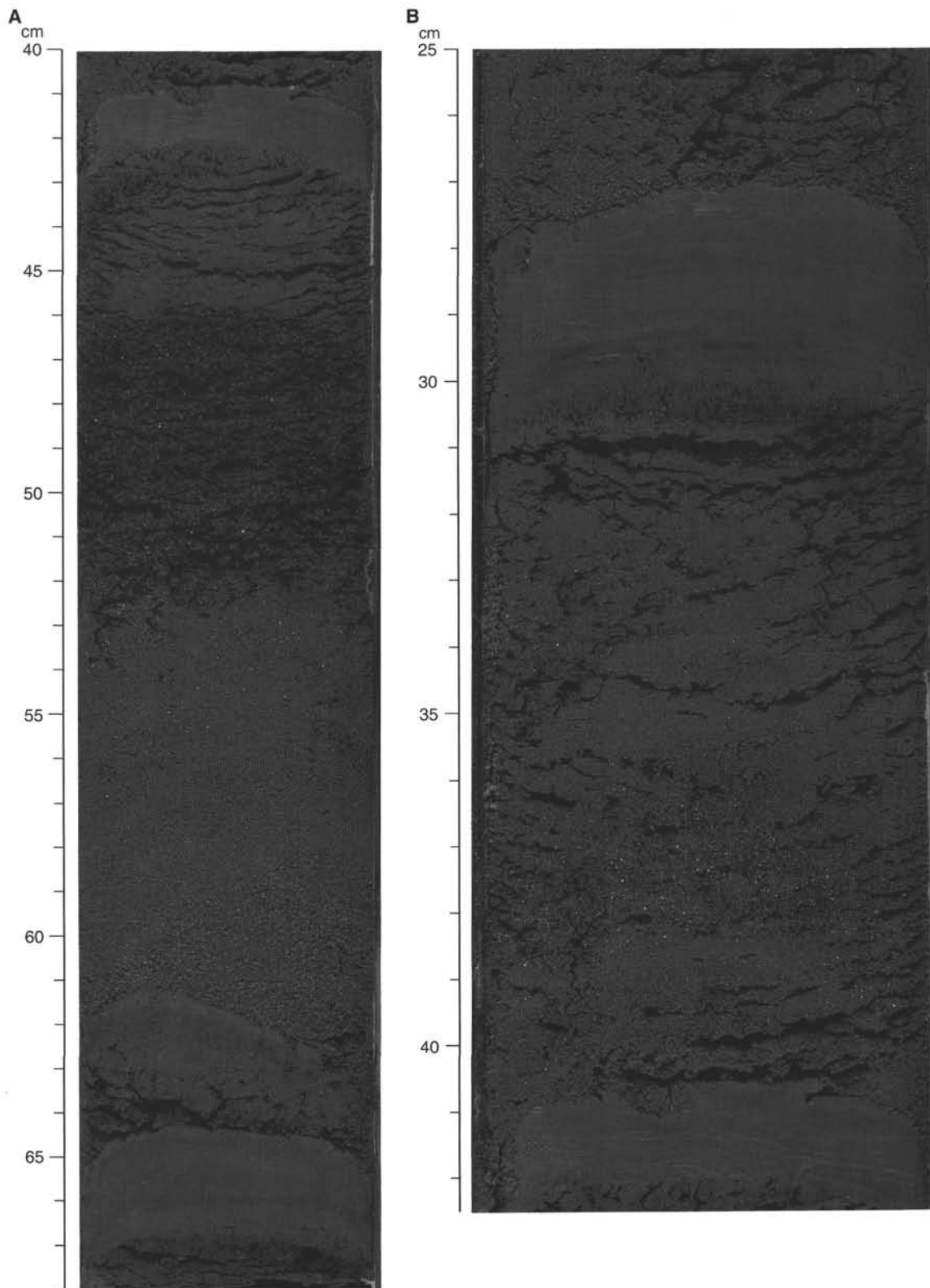


Figure 15. Graded medium bed of sand from Unit III. **A.** 155-945A-7H-1, 40–68 cm. The bed is rich in organic detritus from 46 to 52 cm and grades through silt into clay from 41 to 46 cm. The steeply dipping contact from 59 cm (right) to 61 cm (left) between the medium sand below and the fine sand above is of uncertain depositional origin. **B.** 155-945A-7H-1, 25–42.5 cm. This bed grades upward from predominantly sandy silt (38.5–40.5) through silt and into clay at the top.

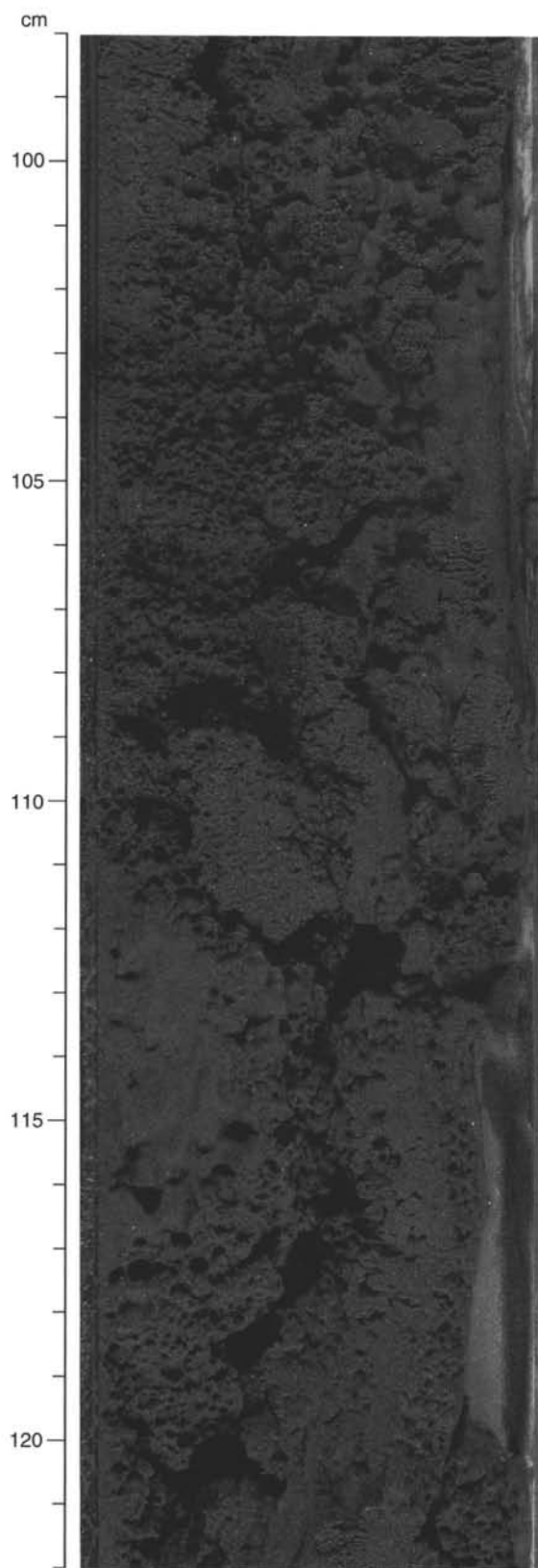


Figure 16. Gas-disrupted sand in Unit III that might have contained a gas hydrate, which melted before opening of the core (155-945A-7H-3, 98–122 cm).

fine sand; however, the lower portion is fine to medium sand with rare coarse grains. The finer grains are angular to subrounded, but the coarse grains are well rounded. The lower 50 cm of this bed appears to contain fewer medium grains and coarse grains than the interval above. Two intervals with mud clasts occur in the upper portion of the bed. A similar bed of sand, approximately 7.4 m thick, occurs at interval 945A-7H-5, 118 cm, through -8H-4, 76 cm. This bed also is composed of fine sand at the top, but the lower half of the bed contains poorly sorted fine to medium sand with rare to common coarse grains and granules <3 mm in diameter. Although some of these thick beds may be attributable to "flow-in," the apparent slight normal grading observed within the thickest beds suggests that disturbance may be minimal.

The two thick sand beds described in the previous paragraph are separated by an 11-m-thick interval of laminae and sand beds of variable thickness (interval 945A-6H-5, 55 cm, through -7H-5, 118 cm; Figs. 5 and 15A, -B). A similar set of beds characterizes interval 945A-8H-4, 76 cm, through -8H-5, 74 cm (Fig. 5). Layers of organic detritus are present in a few of these beds (Fig. 15), and rare intervals with mud clasts occur. A few graded beds show reverse grading in the lower few centimeters, then grade normally upward to the top of the bed. This inverse-to-normal grading has implications for the hydrodynamics of the turbidity currents that deposited these beds; but, at present, the significance of this type of grading is uncertain (e.g., Hiscott, 1994). The basal part of Unit III has two thick, graded sand beds (Fig. 5). In addition to the primary structure, one 2.13-m-thick sand bed has a 50-cm-thick interval in which gas disruption, possibly gas hydrates, created a honeycomb pattern of voids (Fig. 16).

### Mineralogy

Mineralogy was determined by estimation of mineral volume percentages in smear slides and by X-ray diffraction (XRD) analysis of samples from silt laminae, silt beds, and silty clay units (Table 2). Three smear slides of sandy sediment from Unit III were analyzed and have sand:silt:clay ratios of 50:40:10, 80:20:0, and 82:10:8 (Samples 945A-4H-2, 125 cm; 945A-7H-6, 2 cm; and 945A-8H-6, 20 cm). The mean composition of these samples is about 70% quartz, 10% feldspar, 10% heavy minerals, 3% mica, 4% foraminifers, 2% spicules, and 1% organic detritus.

### Spectrophotometry

Reflectance of visible light was low throughout the sediment column recovered at Site 945. Maximum reflectance levels of 35% characterize the brown calcareous clay in Unit I. Reflectance values obtained from the dark olive gray to very dark gray silty clay, clay, silt, and sand beds in Units II and III range between 10% and 25%. The ratio between spectral reflectance values for the red (650–700 nm) and the blue (450–500 nm) spectrum averages 1.18 (Fig. 4). The highest red/blue ratio of 1.7 was measured in the calcareous clay of Unit I, and results from the high content of iron oxyhydroxides. Units II and III have red/blue ratios near the mean for turbidite sediment at other sites from Leg 155. In these units, positive deviations from the mean red/blue ratio are associated with thick, dark grayish brown silt and sand beds containing iron-oxide-stained quartz grains. Red/blue ratios lower than the mean coincide with intervals of dark olive gray clay or sand beds rich in clay clasts.

### Discussion

Hole 945A was drilled into the floor of the Amazon Channel; however, seismic correlation with Site 946 suggests that the channel floor at Site 945 is incised into the pre-existing fan deposits and contains little or no channel-fill deposits. Thus, most of the coarse, thick sand deposits composing Unit III may represent older lower-fan de-

**Table 2. Relative peak intensities of the main minerals in sand and silty clay samples from Unit III in Hole 945A.**

Core, section, interval (cm)	Depth (mbsf)	Relative intensity of primary peaks								
		Smectite	Mica + Illite	Kaolinite	Quartz	Plagioclase	K-feldspar	Augite	Hornblende	Calcite
155-945A-										
3H-1, 120–121	19.70	11.8	25.5	13.7	100	8.6	4.1	2.8	*	*
4H-7, 42–43	37.42	7.2	28.9	16.4	100	10.4	*	2.7	*	*
5H-2, 9–10	39.09	7	17.8	7.4	100	8.8	4.9	2.8	*	*
6H-3, 80–81	50.01	2	2.8	1.6	100	5	2.5	0.4	0.6	*
7H-1, 66–67	57.16	8	16.6	6.1	100	5.3	4	1.3	*	*
8H-5, 18–20	72.18	7.7	16.9	8.5	100	8.5	*	2.6	1.9	*

Notes: See "Lithostratigraphy" section in the "Explanatory Notes" chapter, this volume, for XRD methods. \* = non-detection.

positional lobes deposited prior to the development of this reach of the Amazon Channel (see "Lithostratigraphy" and "Synthesis and Significance" sections, "Site 946" chapter, this volume).

The lower portion of Unit III apparently contains the thickest sand beds recovered at any Leg 155 site; however, the actual thicknesses of these beds may be less than that recovered because of "flow-in" (see above). On the other hand, these thick sand beds appear to show slight normal grading, and wire-line logs through this interval of sand at Site 946 suggest that sand beds up to several meters in thickness are present (see "Downhole Logging" section, "Site 946" chapter, this volume). The graded sand beds recovered appear to represent deposition primarily by turbidity currents; however, the presence of mud clasts and poorly sorted sand in some beds suggests possible deposition by sandy mass flows such as debris flows or liquefied flows that may form the basal, high-density portions of turbidity currents. The abundant organic detritus in many beds, including rare pieces of wood, clearly demonstrates that most sediment was derived from fluvial and deltaic sources. The two thick sand units at the top of Unit III that contain numerous, large, folded and deformed mud clasts may represent debris-flow deposits generated by slumps, possibly through failure of the channel wall up-fan in response to avulsion. Overall, the graded sand beds below 40 mbsf appear to be organized into two thinning- and fining-upward cycles (Fig. 5; intervals 945A-5H-2, 122 cm, through -6H-5, 65 cm, and 945A-6H-5, 65 cm, through -8H-CC, 26 cm).

Unit II consists of a thin deposit of gray hemipelagic silty clay that overlies the channel deposits. This sediment grades upward into the brown, carbonate-rich hemipelagic sediment of Unit I, which apparently records the rather abrupt decrease in terrigenous sediment supply to the entire Amazon Fan in response to sea-level rise at the beginning of the Holocene (e.g., Damuth, 1977) and suggests that the Amazon Channel has been inactive during this time period.

## BIOSTRATIGRAPHY

### Calcareous Nannofossils

Calcareous nannofossils recovered at Site 945 are all from nannofossil Zone CN15b (Table 3). An abundant well-preserved nannofossil assemblage with low diversity is present in the calcareous nannofossil and foraminifer clay in the mud-line sample. Nannofossils are absent in the upper part of Unit II (Sample 945A-1H-1, 56–58 cm) but reappear between 1.04 mbsf and 1.41 mbsf (Samples 945A-1H-1, 104–106 cm; -1H-1, 125–128 cm; and -1H-1, 141–143 cm). This might indicate the presence of a thin resedimented sequence within Unit II.

Nannofossils are absent in Unit III from 3.12 mbsf to 55.55 mbsf (Samples 945A-1H-3, 12–14 cm, through -6H-CC, 19–20 cm). In the lower part of Unit III nannofossils occur in very low abundances from 65.85 mbsf to 75.25 mbsf (Samples 945A-7H-CC, 35–36 cm, through -8H-CC, 25–26 cm). Lighter colored intervals in Unit III at 15.82 mbsf and 38.77 mbsf (Samples 945A-2H-5, 82 cm, and -5H-1, 127 cm) were barren of nannofossils but contained authigenic carbonate particles, possibly siderite.

### Planktonic Foraminifers

The boundary between Ericson Zones Z and Y is tentatively placed between 0.32 mbsf and 0.56 mbsf (Samples 945A-1H-1, 30–32 cm, and -1H-1, 56–58 cm; Table 4; Fig. 17), at the base of Unit I. The occurrence of rare *G. tumida* at 1.23 mbsf (945A-1H-1, 123–125 cm) is considered to be due to reworking.

Planktonic foraminifers occur sporadically in the top of Unit III at 18.5 mbsf, down to a depth of 37.9 mbsf (Samples 945A-2H-CC, 2–11 cm, through -4H-CC, 0–5 cm). The absence of *G. tumida*, *G. menardii*, and *P. obliquiloculata* defines the top of Unit III as the Y

**Table 3. Calcareous nannofossil and siliceous microfossil abundance data for Hole 945A.**

Core, section, interval (cm)	Top interval (mbsf)	Bottom interval (mbsf)	Calcareous nannofossils			Diatoms				Ericson Zone (inferred from foraminifers)	Age (inferred from foraminifers)
			Abundance	Preservation	Zone	Marine	Freshwater	Sponge spicules	Radiolarians		
155-945A-											
1H-MI, 0	0.00		a	g	CN15b	—	—	—	—	Z	Holocene
1H-1, 30–32	0.30	0.32	c	g		—	—	—	—	Z	Holocene
1H-1, 56–58	0.56	0.58	b	—		—	—	—	—	Y	late Pleist.
1H-1, 104–105	1.04	1.05	tr	—		—	—	—	—		
1H-1, 125–128	1.25	1.28	c	g		—	—	—	—		
1H-1, 141–143	1.41	1.43	f	g		—	—	—	—		
1H-3, 12–14	3.12	3.14	b	—		—	—	—	—		
1H-CC, 2–3	9.02	9.03	b	—		—	—	—	—	Y	late Pleist.
2H-5, 82	15.82		b	—		—	—	—	—		
2H-CC, 11–12	18.58	18.59	b	—		—	—	—	—	Y	late Pleist.
4H-CC, 4–5	37.92	37.93	b	—		—	—	—	—		
5H-1, 127	38.77		b	—		—	—	—	—		
5H-CC, 30–31	47.69	47.70	b	—		—	—	—	—	Y	late Pleist.
6H-CC, 19–20	55.55	55.56	b	—		—	—	—	—		
7H-CC, 35–36	65.85	65.86	tr	—		—	—	—	—	Y	late Pleist.
8H-CC, 25–26	75.25	75.26	tr	—		—	—	—	—	Y	late Pleist.

Table 4. Foraminifer abundance data for Hole 945A.

Core, section, interval (cm)	Top interval (mbsf)	Bottom interval (mbsf)	<i>Globorotalia menardii</i>	<i>Globorotalia tumida</i>	<i>Globorotalia tumida flexuosa</i>	<i>Pulleniatina obliquiloculata</i>	<i>Globigerinoides ruber</i> (white)	<i>Globigerinoides ruber</i> (pink)	<i>Globorotalia hexagonus</i>	<i>Neogloboquadrina dutertrei</i>	<i>Globorotalia trilobus trilobus</i>	<i>Globorotalia inflata</i>	<i>Globorotalia truncatulinoides</i>	<i>Globigerina bulloides</i>	<i>Globigerinoides trilobus sacculifer</i>	<i>Globorotalia fimbriata</i>	<i>Bolliella adamsi</i>	<i>Hastigerinella digitata</i>	<i>Globigerina calida calida</i>	<i>Globorotalia crassaformis hessi</i>	<i>Globorotalia crassaformis viola</i>	<i>Globorotalia tosaensis</i>	<i>Globorotalia crassaformis crassaformis</i>	Other planktonic foraminifers	Vivianite nodules	Overall foraminifer abundance	Preservation	Abundance of bathyal benthic foraminifers	Abundance of abyssal benthic foraminifers	Comments	Ericson Zone	Age		
155-945A-																																		
1H-MI, 0	0.00		F	F	B	C	A	F	B	F	C	R	F	B	A	R	B	B	B	B	B	B	B	B	B	A	G	B	B		Z	Holocene		
1H-1, 30-32	0.30	0.32	B	C	B	C	C	F	B	C	B	F	F	B	C	R	B	B	R	B	B	B	B	B	B	A	G	B	B		Z	Holocene		
1H-1, 56-58	0.56	0.58	B	B	B	B	B	B	B	B	B	B	B	B	B	B	B	B	B	B	B	B	B	B	B	B	—	B	B	W, S	?	?		
1H-1, 104-106	1.04	1.06	B	B	B	B	B	B	B	B	B	B	B	B	B	B	B	B	B	B	B	B	B	B	B	B	—	B	B	W, S	?	?		
1H-1, 123-125	1.23	1.25	B	R	B	C	C	F	B	C	C	R	F	B	C	R	B	B	B	B	B	B	B	B	B	A	G	R	B		Y	late Pleist.		
1H-1, 141-143	1.41	1.43	B	B	B	C	C	B	B	F	C	B	B	B	F	B	B	B	B	B	B	B	B	B	B	F	P	B	B		Y	late Pleist.		
1H-CC, 0-3	9.00	9.03	R	B	B	B	F	B	B	F	C	B	B	B	F	B	B	B	B	B	B	B	B	B	B	R	M	B	B	W, S	Y	late Pleist.		
2H-CC, 2-11	18.49	18.58	B	B	B	B	C	F	B	C	C	R	B	B	C	B	B	B	B	B	B	B	B	B	B	A	C	M	B	B	IS, S	Y	late Pleist.	
3H-CC, 43-52	27.22	27.31	B	B	B	B	B	B	B	B	B	B	B	B	B	B	B	B	B	B	B	B	B	B	B	B	—	B	B	S	?	?		
4H-CC, 0-5	37.88	37.93	B	B	B	B	B	B	B	C	C	B	B	B	C	B	B	B	B	B	B	B	B	B	B	R	G	B	B	S	?	?		
5H-CC, 21-30	47.60	47.69	B	B	B	B	B	B	B	B	B	B	B	B	B	B	B	B	B	B	B	B	B	B	B	B	—	B	B	S	?	?		
6H-CC, 10-19	55.46	55.55	B	B	B	B	B	B	B	B	B	B	B	B	B	B	B	B	B	B	B	B	B	B	B	B	G	B	B	S	?	?		
7H-CC, 26-35	65.76	65.85	B	B	B	B	B	B	B	B	B	B	B	B	B	B	B	B	B	B	B	B	B	B	B	B	G	B	B	W, S	?	?		
8H-CC, 16-25	75.16	75.25	B	B	B	B	B	B	B	B	B	B	B	B	B	B	B	B	B	B	B	B	B	B	B	B	G	B	B	W, S	?	?		

Notes: Key to Comments section: Sediment composition: S = sand; indicators of reworking: W = wood fragments, IS = iron-stained foraminifers. Note also the occurrence of bathyal benthic foraminifers.

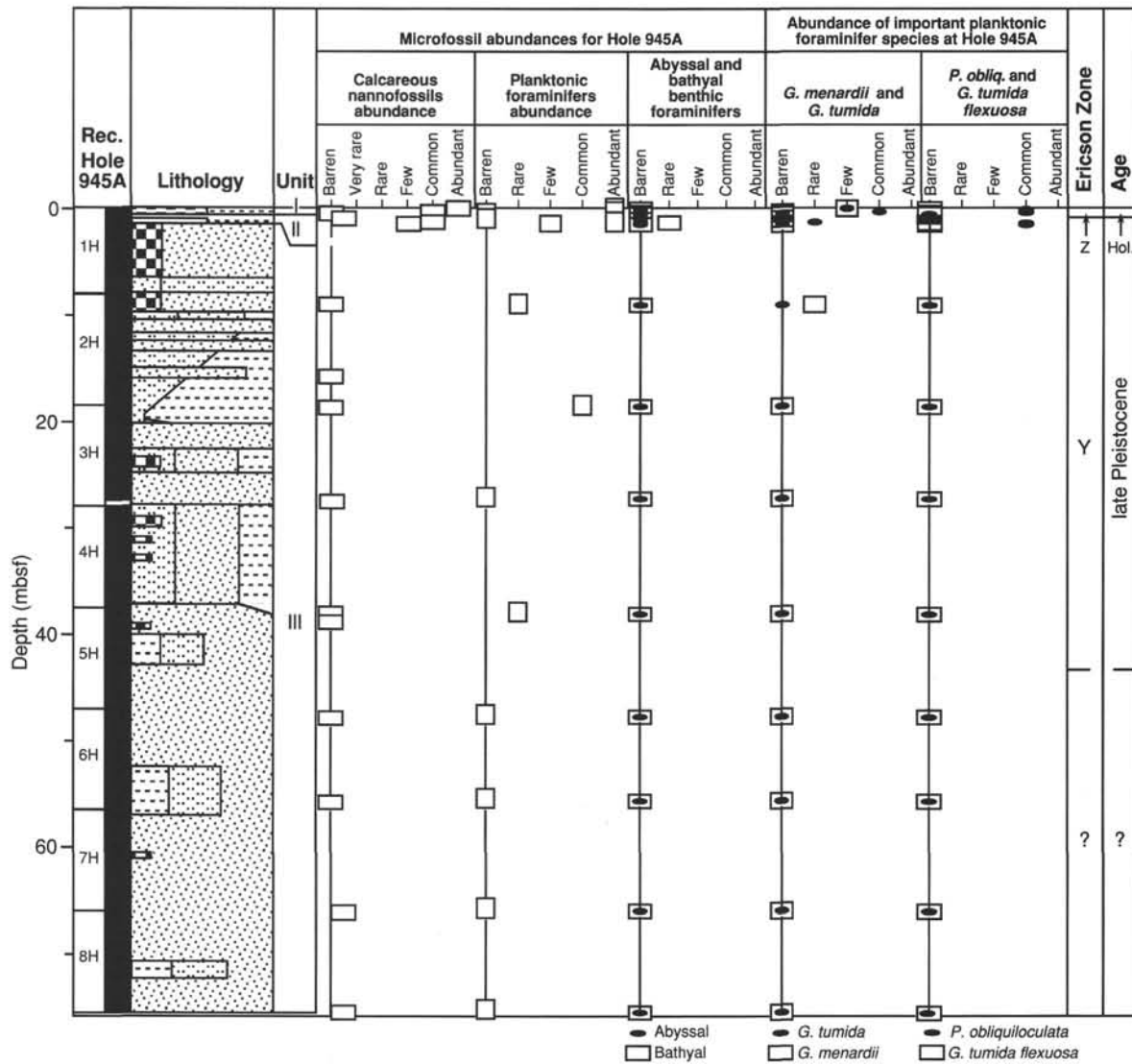


Figure 17. Biostratigraphic summary for Site 945.

Zone, younger than 40 ka. Planktonic foraminifers are absent in the lower part of Unit III between 47.6 mbsf and 75.2 mbsf (Samples 945A-5H-CC, 21–30 cm, through -8H-CC, 16–25 cm). All samples in Unit III contain a high abundance of sand.

**Benthic Foraminifers**

Benthic foraminifers are rare or absent in Hole 945A (Table 4; Fig. 17).

**Siliceous Microfossils**

Rare marine diatoms were observed only in the mud-line sample of Hole 945A.

**Palynology**

Two samples were examined from Hole 945A at 18.58 mbsf and 47.70 mbsf (Samples 945A-2H-CC, 11–12 cm, and -5H-CC, 30–31 cm). Both samples were from the sandy turbidites of Unit III and were found to be barren of pollen and spores. Wood particles were observed in moderate abundance in both samples. Macroscopic wood

fragments (>63 μm) were observed in five other samples between 0.56 mbsf and 75.16 mbsf (Table 4). Dinoflagellates were found at 18.58 mbsf (Sample 945A-2H-CC, 11–12 cm).

**Stratigraphic Summary**

Unit I contains well-preserved nannofossil and planktonic foraminifer assemblages indicative of the Holocene. The nannofossils represent nannofossil Zone CN15b. The boundary between Ericson Zones Z and Y is tentatively placed between 0.32 mbsf and 0.36 mbsf, at the base of Unit I. The top of Unit III has been defined as the Y Zone, younger than 40 ka due to the absence of *G. tumida*, *G. menardii*, and *P. obliquiloculata*. Below a depth of 47.6 mbsf in Unit III, planktonic foraminifers are absent. Nannofossils are very rare or absent in Unit III.

**PALEOMAGNETISM**

**Remanence Studies**

Selected archive-half sections from seven APC cores were measured on the cryogenic pass-through magnetometer. Only Core

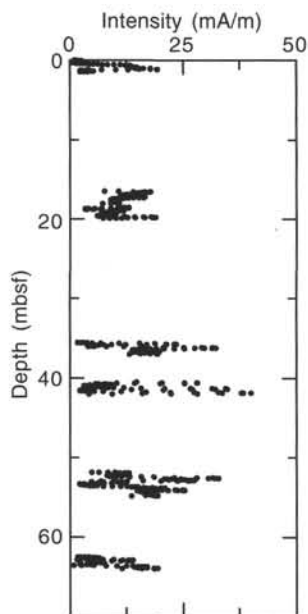


Figure 18. Remanence intensity, after AF demagnetization to 20 mT, for Hole 945A.

945A-8H was not measured as it mostly consisted of soupy sand and silt. Cores 945A-3H through -8H were oriented with the Tensor tool, which appears to have performed well. Because of the predominantly silty and sandy nature of these cores, records of geomagnetic secular variation or of excursions could not be discerned. The highest remanence intensity in the measured core sections occurs at ~42 mbsf in Core 945A-5H (Fig. 18).

### Magnetic Susceptibility Studies

Whole-core magnetic and discrete-sample susceptibilities were measured on all cores collected from Site 945. Both data sets show similar trends downhole (Fig. 19). Discrete sample measurements show that the sand beds in Unit III have higher susceptibilities than the finer silt and clay. The lowest values are within carbonate-rich Unit I.

## ORGANIC GEOCHEMISTRY

### Volatile Hydrocarbons

Headspace methane concentrations increase rapidly below the sediment surface to 29,000 ppm at 16.50 mbsf (Table 5; Fig. 20). Methane concentrations below this depth range from ~13,000 ppm at 20.00 mbsf to 5400 ppm at 62.50 mbsf. The vacutainer methane concentration for a gas void sampled at 40.50 mbsf in Hole 945A is 134,000 ppm. Higher molecular weight hydrocarbons were not detected, indicating a predominantly biogenic methane source at Site 945.

### Carbon, Nitrogen, and Sulfur Concentrations

Carbonate (calculated as CaCO<sub>3</sub>) concentrations in Hole 945A range from 0.6% at 61.90 mbsf to 3.2% at 17.62 mbsf (Table 6; Fig. 21). The carbonate-rich Unit I (0–0.45 mbsf) was not sampled. TOC concentrations range between 0.65% and 1.3%. Two low values (<0.05%) were measured in fine sand layers at 10.62 and 61.90 mbsf. Two relatively high values (>1.2%) were measured in clay intervals at 17.62 and 52.60 mbsf. TN concentrations range from 0.07% to

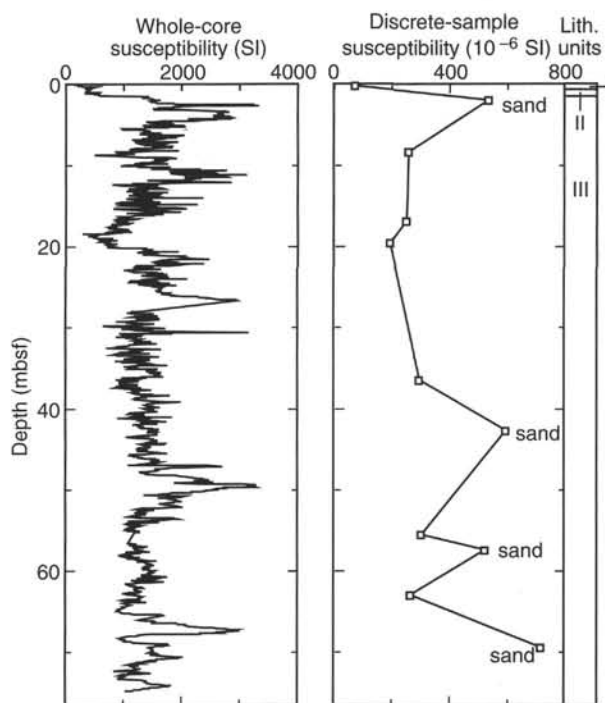


Figure 19. Whole-core and discrete-sample susceptibilities for Hole 945A. The discrete samples containing sand are labeled on the figure.

Table 5. Gas concentrations in sediments from Site 945.

Core, section, interval (cm)	Depth (mbsf)	Sed. temp.* (°C)	Methane	
			HS (ppm)	VAC (ppm)
155-945A-				
1H-5, 0-5	5.90	2	2	
2H-6, 0-5	16.50	3	28,945	
3H-2, 0-5	20.00	3	13,098	
4H-4, 0-5	32.50	3	13,137	
5H-3, 0-5	40.50	3	9,793	134,227
6H-6, 0-5	53.34	4	8,645	
7H-5, 0-5	62.50	4	5,388	
8H-5, 0-5	72.00	4	5,895	

Notes: HS = headspace; VAC = vacutainer. \*Assumed geothermal gradient = 32°C/km. Bottom-water temperature = 2°C.

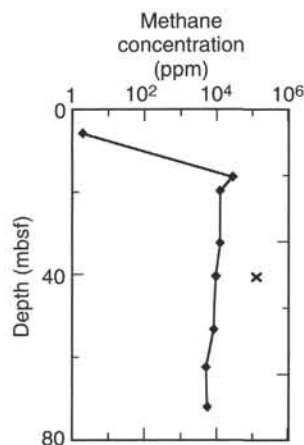


Figure 20. Methane concentrations at Site 945. Headspace (diamond) and vacutainer (x) samples are plotted.

Table 6. Elemental and organic carbon compositions of sediments from Site 945.

Core, section, interval (cm)	Depth (mbsf)	IC (%)	CaCO <sub>3</sub> * (%)	TC (%)	TOC (%)	TN (%)	TS (%)	[C/N]a	Lithology
155-945A-									
1H-6, 63-64	8.03	0.21	1.7	1.08	0.87	0.09	0.20	11	Silty clay
2H-2, 12-13	10.62	0.08	0.7	0.08	0.00	0.01	0.06	0	Fine sand
2H-6, 112-113	17.62	0.39	3.2	1.61	1.22	0.12	0.14	12	Clay
3H-1, 98-99	19.48	0.33	2.7	0.98	0.65	0.12	0.05	7	Silty clay
4H-4, 75-76	33.25	0.34	2.8	1.04	0.70	0.12	0.01	7	Silty clay
6H-5, 68-69	52.52	0.21	1.7	1.13	0.92	0.07	0.05	15	Clay
6H-5, 76-77	52.60	0.37	3.1	1.67	1.30	0.13	0.12	12	Silt
7H-2, 8-9	58.08	0.15	1.2	0.99	0.84	0.12	0.03	8	Clay
7H-4, 90-91	61.90	0.07	0.6	0.11	0.04	0.03	0.00	2	Fine sand

Note: \* = calculated assuming all IC is calcite.

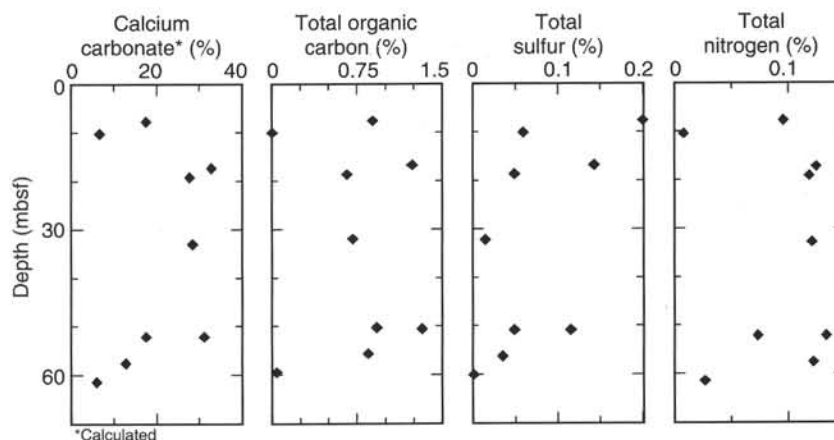


Figure 21. Concentration profiles of carbonate, total organic carbon, total sulfur, and total nitrogen in Hole 945A.

Table 7. Interstitial water chemistry, Site 945.

Core, section, interval (cm)	Depth (mbsf)	Salinity	pH	Alkalinity (mM)	Cl <sup>-</sup> (mM)	Mg <sup>2+</sup> (mM)	Ca <sup>2+</sup> (mM)	K <sup>+</sup> (mM)	HPO <sub>4</sub> <sup>2-</sup> (μM)	SO <sub>4</sub> <sup>2-</sup> (mM)	NH <sub>4</sub> <sup>+</sup> (mM)	H <sub>4</sub> SiO <sub>4</sub> (μM)	Na <sup>+</sup> (mM)	Fe <sup>2+</sup> (μM)	Mn <sup>2+</sup> (μM)
155-945A-															
1H-4, 145-150	5.95	34.5	7.51	8.79	552	49.8	10.2	11.0	33.1	23.3	1.5	450	475	62.1	18.4
2H-5, 145-150	16.45	33.0	7.60	15.08	552	41.2	5.4	8.9	11.9	0.4	4.1	376	462	18.2	2.8
3H-1, 150-155	19.95	32.0	7.56	10.77	555	40.7	5.1	8.3	3.8	0.5	4.3	242	462	22.3	3.4
4H-3, 145-150	32.45	33.0	7.56	10.64	556	41.8	5.9	8.0	7.7	0.2	4.2	344	459	42.0	4.4
5H-2, 145-150	40.45	32.0	7.43	9.06	559	41.8	5.8	6.9	5.8	0.2	3.3	408	464	43.7	4.5
8H-4, 140-150	71.90	32.0	7.53	12.02	560	39.9	5.2	8.8	19.4	0.6	3.0	367	471	14.9	3.2

0.12% in most of the samples of Hole 945A, with two low values in the sand layers that have low TOC content. TS is low (<0.25%) throughout this site.

All samples from Hole 945A correspond to Unit III. The major variations in bulk elemental compositions at this site are associated with changes in grain size. The [C/N]a ratios range from 7 to 15, except in the two previously described sand layers where the [C/N]a is very low due to the extremely low organic carbon content.

## INORGANIC GEOCHEMISTRY

### Interstitial Water Analysis

Interstitial water samples were collected from six sediment samples at Hole 945A (Table 7; Fig. 22). Five samples were taken from the upper 40.45 mbsf and one sample from 71.90 mbsf. The sample spacing varied due to poor recovery in sandy sediment.

Salinities of the water samples range from 32.0 to 34.5 (Fig. 22A). The salinity decreases from 34.5 at 5.95 mbsf to 33.0 at 16.50 mbsf, and remains between 32.0 and 33.0 downhole. Chloride concentrations increase gradually throughout the hole, from 552 mM at 5.95

mbsf to 560 mM at 71.90 mbsf (Fig. 22B). Pore-water pH values fall into a narrow range, from 7.43 to 7.60 (Fig. 22C) with no clear downhole trend. Pore-water alkalinity increases from 8.79 mM at 5.95 mbsf to 15.08 at 16.45 mbsf, and then decreases to 10.77 mM by 19.95 mbsf. Below 19.95 mbsf, alkalinity remains between 9.06 and 12.02 mM (Fig. 22D). Dissolved magnesium and calcium concentrations decrease from 49.8 mM and 10.2 mM, respectively, at 5.95 mbsf to 41.2 and 5.4 mM by 16.45 mbsf (Fig. 22E, -F). Thereafter, concentrations are relatively uniform, with Mg varying between 39.9 and 41.8 mM, and Ca between 5.1 and 5.9 mM. Pore-water sulfate concentrations decrease from 23.3 mM at 5.95 mbsf to zero by 16.45 mbsf, and remain near zero downhole (Fig. 22G).

Ammonium concentrations increase from 1.5 mM at 5.95 mbsf to 4.1 mM at 16.45 mbsf (Fig. 22H). Values remain between 4.1 and 4.3 mM until 32.45 mbsf. The two lowermost samples have concentrations of 3.3 and 3.0 mM. Pore-water phosphate concentrations are 33.1 μM in the shallowest sample at 5.95 mbsf. Concentrations decrease to 11.9 by 16.45 mbsf and remain between 3.8 and 19.4 μM for the remainder of the hole (Fig. 22I). Dissolved silica concentrations vary from 242 to 450 μM, with no clear downhole trend (Fig. 22J). Dissolved potassium decreases gradually downhole from 11.0

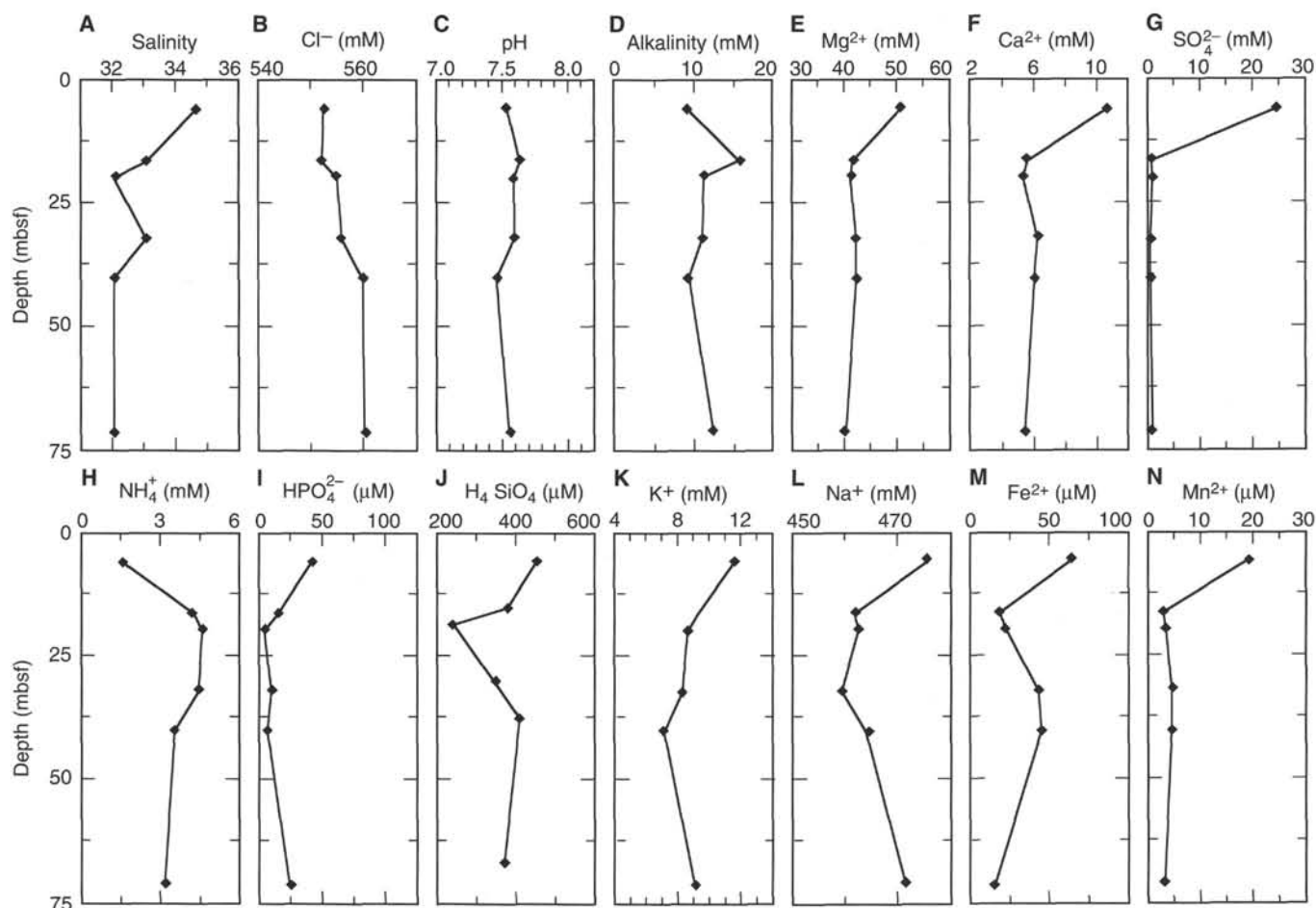


Figure 22. Downhole variation in pore-water chemistry. A. Salinity. B. Chloride. C. pH. D. Alkalinity. E. Magnesium. F. Calcium. G. Sulfate. H. Ammonium. I. Phosphate. J. Silica. K. Potassium. L. Sodium. M. Iron. N. Manganese.

mM at 5.95 mbsf to 6.9 mM at 40.45 mbsf (Fig. 22K). The concentration then increases slightly to 8.8 mM at 71.90 mbsf. Sodium concentrations decrease from 475 mM at 5.95 mbsf to 462 mM at 16.45 mbsf, and remain between 459 and 464 mM through 40.45 mbsf (Fig. 22L). At 71.90 mbsf the concentration increases to 471 mM. Dissolved iron concentrations are highest in the uppermost sample, 62.1 μM at 5.95 mbsf, and then decrease to 18.2 μM at 16.45 mbsf. Concentrations are slightly higher in the interval 32.45–40.45 mbsf, between 42.0 and 43.7 μM, and then decrease to 14.9 μM in the lowermost sample (Fig. 22M). Manganese concentrations decrease from 18.4 μM in the sample at 5.95 mbsf to 2.8 μM at 16.45 mbsf and remain between 3.2 and 4.4 μM for the remainder of the hole (Fig. 22N).

Although overall the pore-water chemistry at this site is similar to that at previous sites of this leg, there are several slight differences. The depth to total sulfate reduction appears to be deeper than at most sites. Also, ammonium concentrations peak at lower values than previously observed. This may be due to the sandy nature of the sediment.

## PHYSICAL PROPERTIES

Physical property measurements were conducted on both whole-round core sections and on discrete samples from split cores from Hole 945A. GRAPE density, compressional-wave velocity, and nat-

ural gamma-ray radiation were measured on whole-round cores. Expansion of methane gas commonly affected the sediment, and whole-round measurements were particularly influenced by the expansion. A significant part of the thick sand intervals recovered in Hole 945A is most likely flow-in. As a result of this flow-in, measurements in these intervals are probably not representative of in-situ conditions.

## Index Properties

Index properties were determined for undisturbed, predominantly clayey sediment in Hole 945A (Table 8). Measurements in sand were limited to grain density determinations. Only one sample for index properties was taken from each of the upper two lithologic units in Hole 945A. The water contents measured for Unit I (0–0.45 mbsf) and Unit II (0.45–1.46) are 50% and 64% (Fig. 23). Unusually low water content (29%–37%) characterizes silty clay clasts of the thick sand bed contained within Sections 945A-1H-2 through -1H-6. The water content of these clasts is about 5% to 15% less than it is in silty clay at similar depths at other Leg 155 sites. Below 12 mbsf, the water content profile (for the silty clay) is more typical of those determined at previous Amazon Fan sites, decreasing gradually from 40% at 12.45 mbsf to 30% near the base of the hole.

Grain density varies within a narrow range, 2.65 to 2.81 g/cm<sup>3</sup> (Fig. 23). The average grain density measured for sand, 2.70 g/cm<sup>3</sup>, is only slightly lower than that of silty clay samples, 2.74 g/cm<sup>3</sup>. The grain density decreases gradually with depth as a result of the down-

Table 8. Index properties at Site 945.

Core, section, interval (cm)	Depth (mbsf)	Water content (%)	Wet-bulk density (g/cm <sup>3</sup> )	Grain density (g/cm <sup>3</sup> )	Dry-bulk density (g/cm <sup>3</sup> )	Porosity (%)	Void ratio
155-945A-							
1H-1, 34-36	0.34	49.8	1.52	2.78	0.76	72.9	2.69
1H-1, 94-96	0.94	63.8	1.35	2.77	0.49	82.7	4.77
1H-2, 57-59	2.07			2.74			
1H-3, 6-8	2.96	36.5	1.73	2.67	1.10	60.0	1.50
1H-4, 138-140	5.78	28.9	1.88	2.75	1.34	52.1	1.09
1H-5, 121-123	7.11	33.4	1.80	2.73	1.20	57.1	1.33
1H-6, 68-70	8.08	36.2	1.74	2.76	1.11	60.4	1.53
2H-2, 85-87	11.35			2.71			
2H-3, 45-47	12.45	39.6	1.69	2.81	1.02	64.2	1.80
2H-5, 42-44	15.42	39.8	1.68	2.76	1.01	64.1	1.78
2H-6, 123-125	17.73	36.0	1.75	2.74	1.12	60.0	1.50
2H-7, 19-21	18.19	37.3	1.72	2.76	1.08	61.6	1.60
3H-1, 90-92	19.40	38.8	1.70	2.78	1.04	63.2	1.72
3H-2, 122-124	21.22			2.69			
3H-3, 116-118	22.66	31.0	1.85	2.73	1.27	54.6	1.20
3H-4, 61-63	23.61	28.9	1.90	2.78	1.35	52.4	1.10
3H-5, 78-80	25.28			2.71			
4H-1, 105-107	29.05			2.67			
4H-2, 32-34	29.82	35.4	1.75	2.69	1.13	59.0	1.44
4H-4, 22-24	32.72			2.70			
4H-5, 86-88	34.86	32.7	1.81	2.73	1.22	56.3	1.29
4H-6, 72-74	36.22	29.6	1.88	2.69	1.32	52.5	1.10
4H-7, 24-26	37.24	31.5	1.84	2.76	1.26	55.3	1.24
5H-1, 72-74	38.22			2.65			
5H-2, 72-74	39.72			2.69			
5H-3, 60-62	41.10	30.3	1.87	2.73	1.30	53.7	1.16
5H-4, 69-71	42.69			2.70			
5H-5, 4-6	43.54	29.4	1.91	2.77	1.35	53.0	1.13
5H-6, 14-16	45.14			2.67			
5H-7, 78-80	47.28			2.68			
6H-1, 33-35	47.33			2.72			
6H-2, 83-85	48.54			2.71			
6H-3, 83-85	50.04			2.69			
6H-4, 76-78	51.47			2.65			
6H-5, 134-136	53.18	27.6	1.92	2.71	1.39	50.2	1.01
6H-6, 80-82	54.14	30.1	1.87	2.75	1.31	53.6	1.15
6H-7, 43-45	55.27			2.77			
7H-1, 72-74	57.22			2.72			
7H-2, 13-15	58.13	29.4	1.87	2.68	1.32	52.2	1.09
7H-3, 72-74	60.22			2.71			
7H-4, 27-29	61.27			2.69			
7H-5, 84-86	63.34			2.70			
7H-5, 113-115	63.63	32.3	1.84	2.72	1.24	55.9	1.27
8H-1, 82-84	66.82			2.72			
8H-2, 84-86	68.34			2.69			
8H-3, 85-87	69.85			2.67			
8H-4, 96-98	71.46	28.2	1.92	2.69	1.38	50.7	1.03
8H-5, 56-58	72.56	30.2	1.92	2.78	1.34	54.0	1.18
8H-5, 141-143	73.41			2.70			
8H-6, 113-115	74.63			2.66			

hole increase in sand. As a consequence of the low variability in grain density, variations of porosity and wet-bulk density closely match the water content fluctuations (Fig. 23). Porosity decreases downhole from 83% at 0.94 mbsf to 30% near the base of Hole 945A. The corresponding wet-bulk density increase is from 1.35 to 1.92 g/cm<sup>3</sup>.

There is good agreement between the GRAPE bulk density and the discrete-sample wet-bulk density in the upper 2 mbsf (Fig. 23). The difference between measurements in Unit I most likely results from the sediment not completely filling the core liner. Below 2 mbsf, the densities diverge as a result of gas expansion, and the GRAPE measurements typically are 0.20 to 0.40 g/cm<sup>3</sup> less than the discrete-sample values. Thick sand beds cored in Hole 945A are represented by intervals of distinctly higher density on the GRAPE profile. Densities measured in these intervals are probably not representative of in-situ densities as a result of flow-in.

### Compressional-wave Velocity

Compressional-wave velocity was measured for one sample from Unit II using the DSV and for the interval between 0 and 11.80 mbsf using the PWL. Longitudinal and transverse velocities of 1500 and 1495 m/s, respectively, were measured with the DSV for silty clay from 0.98 mbsf. Transverse velocities determined with the PWL av-

erage 1469 m/s for 0 to 1.46 mbsf (Units I and II) and 1536 m/s between 1.46 and 11.80 mbsf.

### Shear Strength

Measurements of undrained shear strength were made using the motorized shear vane on cores from predominantly silty clay intervals in Hole 945A (Table 9). Shear strengths measured in Units I and II are 8.8 and 5.8 kPa, respectively (Fig. 24). Higher strengths, ranging from 31.8 to 75.5 kPa, are displayed by the clasts in the thick sand bed at the top of Unit III. Below this bed, shear strength is moderately variable and increases only slightly downhole, from 39.5 kPa at 8.08 mbsf to 46.8 kPa at 72.53 mbsf. The range in undrained shear strength over this interval is 19.5 to 53.0 kPa.

### Resistivity

Longitudinal resistivity increases downhole in Hole 945A from approximately 0.22  $\Omega$ m near the seafloor to 0.56  $\Omega$ m near the base of the hole (Table 10; Fig. 25). The resistivity increase parallels the downhole porosity decrease, with most of the change occurring between the seafloor and 36 mbsf. From 36 mbsf to the base of the hole, most of the measurements are clustered between 0.45 and 0.50  $\Omega$ m.

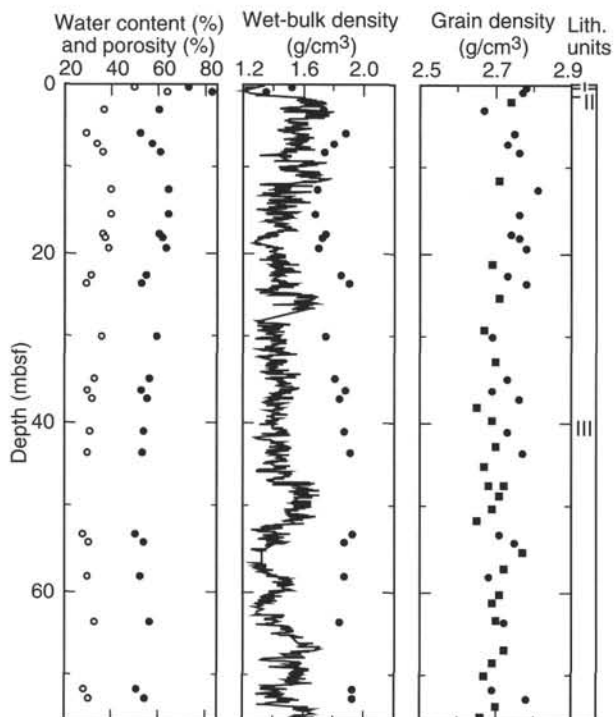


Figure 23. Water content (open circles) and porosity (solid circles), wet-bulk density as determined for discrete samples (circles) and by the GRAPE (line), and grain density in Hole 945A. Silty clay (circles) and silt and sand (squares) sampled only for grain density.

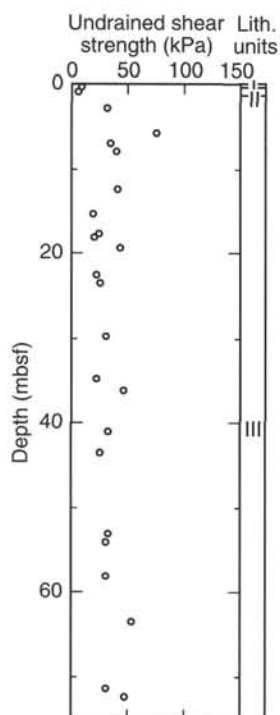


Figure 24. Undrained shear strength in Hole 945A.

Table 9. Undrained shear strength at Site 945.

Core, section, interval (cm)	Depth (mbsf)	Peak undrained shear strength (kPa)	Residual undrained shear strength (kPa)
155-945A-			
1H-1, 34	0.34	8.8	6.0
1H-1, 95	0.95	5.8	4.5
1H-3, 7	2.97	31.8	17.9
1H-4, 138	5.78	75.5	
1H-5, 122	7.12	35.0	19.2
1H-6, 68	8.08	39.5	20.9
2H-3, 46	12.46	40.5	20.1
2H-5, 43	15.43	19.5	
2H-6, 124	17.74	24.0	16.1
2H-7, 19	18.19	19.8	12.2
3H-1, 91	19.41	42.7	21.5
3H-3, 116	22.66	22.1	13.9
3H-4, 62	23.62	25.5	15.9
4H-2, 34	29.84	30.6	17.3
4H-5, 87	34.87	22.6	
4H-6, 73	36.23	45.8	31.2
5H-3, 61	41.11	32.4	17.4
5H-5, 5	43.55	25.2	17.4
6H-5, 135	53.19	32.4	22.0
6H-6, 81	54.15	30.9	21.5
7H-2, 14	58.14	30.9	21.2
7H-5, 114	63.64	53.0	29.0
8H-4, 97	71.47	30.9	18.5
8H-5, 53	72.53	46.8	26.8

Comparison of the longitudinal and transverse resistivities shows that sediments of Units I and II are nearly isotropic, the mud clasts from the upper part of Unit III display positive anisotropy, and most of the silty clay in Unit III is characterized by negative anisotropy. The magnitude of the anisotropy of the silty clay increases downhole in Unit III to a maxima of approximately  $-17\%$  near the base of the hole.

## SYNTHESIS AND SIGNIFICANCE

### Stratigraphic Synthesis

#### *Holocene to Latest Pleistocene Bioturbated Sediment (Units I and II)*

Unit I (0–0.45 mbsf) is a bioturbated Holocene nannofossil-foraminifer clay. An iron-rich crust occurs at the base of the unit. Unit II (0.45–1.46 mbsf) consists of mottled, slightly bioturbated olive-gray mud (Fig. 26).

#### *Possible Avulsion Sand Deposit at the Base of the Channel (Top of Unit III)*

The stratigraphic section at Site 946 shows that the channel at Site 945 is incised at least 30 m into older sediment. The 8-m-thick sand bed with abundant folded mud clasts at the top of Unit III is probably a channel-fill deposit. The water content of these clasts is about 10% lower than for normally consolidated mud at this sub-bottom depth and is more typical of sediment at 30 mbsf. The clasts are set in a matrix of medium sand, whereas the upper part of the graded bed is fine sand. This bed is lithologically similar to that at 58–63 mbsf at Site 943, which also contains large numbers of mud clasts and was interpreted to represent the first deposit following an avulsion. The erosive nature of the channel presumably results from the increase in channel gradient that follows avulsion (Pirmez and Flood, this volume).

Table 10. Electrical resistivity at Site 945.

Core, section, interval (cm)	Depth (mbsf)	Longitudinal resistivity ( $\Omega$ m)	Transverse resistivity ( $\Omega$ m)
155-945A-			
1H-1, 34	0.34	0.217	0.216
1H-1, 94	0.94	0.231	0.229
1H-3, 6	2.96	0.259	0.272
1H-4, 138	5.78	0.318	0.331
1H-5, 122	7.12	0.295	0.301
1H-6, 68	8.08	0.316	0.313
2H-3, 46	12.46	0.302	0.294
2H-5, 43	15.43	0.326	0.311
2H-6, 123	17.73	0.366	0.360
2H-7, 19	18.19	0.380	0.355
3H-1, 91	19.41	0.335	0.317
3H-3, 116	22.66	0.368	0.362
3H-4, 61	23.61	0.372	0.383
4H-2, 33	29.83	0.358	0.360
4H-5, 87	34.87	0.382	0.376
4H-6, 73	36.23	0.458	0.442
4H-7, 25	37.25	0.452	0.426
5H-3, 61	41.11	0.450	0.416
5H-5, 5	43.55	0.479	0.472
6H-5, 135	53.19	0.473	0.425
6H-6, 81	54.15	0.439	0.379
7H-2, 14	58.14	0.475	0.436
7H-5, 114	63.64	0.437	0.399
8H-4, 97	71.47	0.558	0.472
8H-5, 57	72.57	0.492	0.471

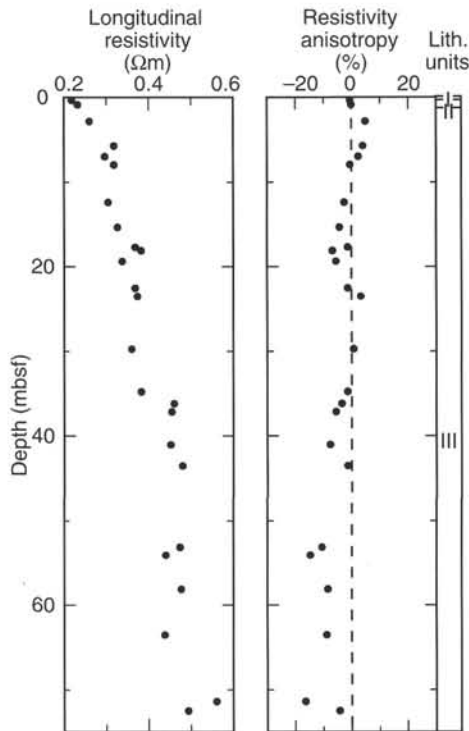


Figure 25. Longitudinal resistivity and resistivity anisotropy in Hole 945A.

**Last-glacial Lower Fan (Unit III)**

Unit III below 10 mbsf consists of medium- to thick-bedded sand interbedded with mud and thin-bedded sand and silt. These beds correlate with Site 946 (see back-pocket foldout) and are discussed in more detail in that chapter. The unit is interpreted as lower fan deposits across which the channel-levee system has prograded. Most of the

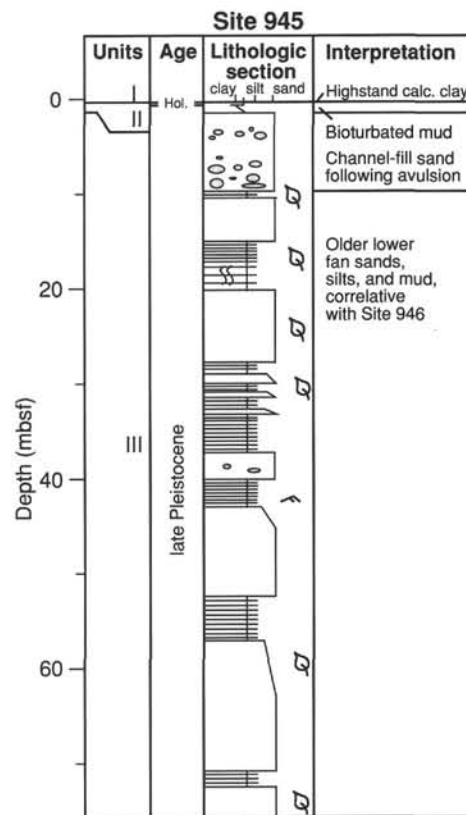


Figure 26. Summary of Site 945 showing (left to right) lithologic units, age, schematic lithologic column, and interpreted sediment facies.

sand is very fine to fine grained, but some beds contain abundant medium sand with rare to common coarse grains and rare granules. Most sand beds are graded. Many of the thicker beds contain angular to well-rounded clasts of mud. Layers of organic detritus occur in some sand. An interval of bioturbated mud occurs at 19–20 mbsf. In the lower part of the unit, sand beds appear to be organized in two thinning-upward sequences, from 76 to 53 mbsf and 53 to 40 mbsf.

**Implications**

Foraminifers and nannofossils range from abundant to few in Units I and II. The boundary between Ericson Zone Z and Y is near the base of Unit II (1.4 mbsf). Rare nannofossils and foraminifers are found in a few samples from Unit III. *P. obliquiloculata* is absent, suggesting an age <40 ka for the upper part of Unit III that contains foraminifers.

The sedimentological significance of the lower fan sand at this site is discussed in the “Synthesis and Significance” section of the “Site 946” chapter (this volume). There is a considerable sedimentary hiatus at the top of Unit III, represented by incision of 30 m into older sediment and deposition of about 18 m of sediment on the adjacent levee. The process of avulsion results in the new channel being steeper than the old one. The resulting acceleration of turbidity currents through new distributary channels leads to little net accumulation.

The depth of total sulfate reduction is 16 mbsf, rather deeper than at most Leg 155 sites. It is unclear whether this is a consequence of the sandy character of the near-surface sediment or the lack of very young sediment other than the Holocene drape.

## REFERENCES\*

- Damuth, J.E., 1977. Late Quaternary sedimentation in the western equatorial Atlantic. *Geol. Soc. Am. Bull.*, 88:695-710.
- Flood, R.D., Manley, P.L., Kowsmann, R.O., Appi, C.J., and Pirmez, C., 1991. Seismic facies and late Quaternary growth of Amazon submarine

- fan. In Weimer, P., and Link, M.H. (Eds.), *Seismic Facies and Sedimentary Processes of Submarine Fans and Turbidite Systems*: New York (Springer), 415-433.
- Hiscott, R.N., 1994. Traction-carpet stratification in turbidites: fact or fiction? *J. Sediment. Res., Sect. A*, 64:204-208.
- Pirmez, C., 1994. Growth of a submarine meandering channel-levee system on the Amazon Fan [Ph.D. thesis]. Columbia Univ., New York.

\*Abbreviations for names of organizations and publications in ODP reference lists follow the style given in *Chemical Abstracts Service Source Index* (published by American Chemical Society).

Ms 155IR-121

**NOTE: For all sites drilled, core-description forms ("barrel sheets") and core photographs can be found in Section 4, beginning on page 703. Forms containing smear-slide data can be found in Section 5, beginning on page 1199. GRAPE, index property, magnetic susceptibility, and natural gamma data are presented on CD-ROM (back pocket).**